

SPARSE SYSTEM IDENTIFICATION BY LOW-RANK APPROXIMATION

FREDY VIDES

ABSTRACT. In this document, some general results in approximation theory and matrix analysis with applications to sparse identification of time series models and nonlinear discrete-time dynamical systems are presented. The aforementioned theoretical methods are translated into algorithms that can be used for sparse model identification of discrete-time dynamical systems, based on structured data measured from the systems. The approximation of the state-transition operators that are determined primarily by matrices of parameters to be identified based on data measured from a given system, is approached by identifying conditions for the existence of low-rank approximations of submatrices of the trajectory matrices corresponding to the measured data, that can be used to compute approximate sparse representations of the matrices of parameters. One of the main advantages of the low-rank approximation approach presented in this document, concerns the parameter estimation for linear and nonlinear models where numerical or measurement noise could affect the estimates significantly. Prototypical algorithms based on the aforementioned techniques together with some applications to approximate identification and predictive simulation of time series models with symmetries and nonlinear structured dynamical systems in theoretical physics, fluid dynamics and weather forecasting are presented.

1. INTRODUCTION

In this document, some structured matrix approximation problems that arise in the fields of system identification and model order reduction of large-scale structured dynamical systems are studied.

The main purpose of this document is to present some theoretical and computational techniques that have been developed for the approximate structure preserving sparse identification of discrete-time dynamical systems based on structured data measured from the systems. In particular, we explore the idea of using low-rank approximations of submatrices of the Hankel-type trajectory matrices corresponding to the data samples, for the computation of the approximate sparse representations of the matrices of parameters to be identified as part of the model identification processes considered in this document.

As part of the process previously described, some general results in approximation theory and matrix analysis with applications to sparse identification of time series models and nonlinear dynamical systems are obtained. The approximation of the corresponding state-transition operators determined by matrices of parameters to be identified, is approached by identifying conditions for the existence of easily computable integers that can be applied to estimate the computability of approximate sparse representations of the matrices of parameters, and as a by-product of the computation of these numbers one obtains low-rank approximations of submatrices of the trajectory matrices corresponding to some data measured from the system under study, that can be used to compute the sparse approximants of the matrices of parameters.

One of the main advantages of the low-rank approximation approach presented in this document, concerns the parameter estimation for linear and nonlinear models where numerical or measurement noise could affect the estimates significantly. Another advantage is the reduction of arithmetic complexities obtained as a consequence of the application of low-rank approximation techniques, as studied by Chen, Avron and Sindhvani in [7] in the context of scalable nonparametric learning. The low-rank

Date: August 4, 2021.

2010 Mathematics Subject Classification. Primary 93B28, 47N70; Secondary 93C57, 93B40.

Key words and phrases. System identification, low-rank approximation, time series, equivariant system.

approximation approach implemented in this study makes sparse linear least squares solver algorithms like algorithm 1, suitable for parallelization.

The identification and predictive numerical simulation of the evolution laws for discrete-time systems are highly important in predictive data analytics, for models related to the automatic control of systems and processes in science and engineering in the sense of [5, 2, 23]. Part of the motivation for the development of the techniques presented in this paper came from matrix approximation problems that arise in the fields of system identification in the sense of [30, 22, 26], and the computation of digital twins as considered in [33, 32].

The study reported in this document was inspired by the theoretical and computational questions and results presented by Salova, Emenheiser, Rupe, Crutchfield, and D’Souza in [26], by Boutsidis and Magdon-Ismael in [3], by Finzi, Stanton, Izmailov and Wilson in [12], by Brockett and Willsky in [4], by Moskvina and Schmidt in [22], by Shmid in [28], by Proctor, Brunton and Kutz in [23], by Kaiser, Kutz and Brunton in [18], by Kaheman, Kutz and Brunton in [17], by Freedman and Press in [14], by Franke and Selgrade in [13], by Farhood and Dullerud in [11], by Schaeffer, Tran, Ward and Zhang in [27], and by Loring and Vides in [21].

Among the previous references, from a computational perspective, two key sources of inspiration for the work reported in this document were the amazing computational implementations of **SINDy** and Douglas-Rachford algorithms for sparse nonlinear system identification along the lines of [6], [17] and [27]. One of the objectives of the work reported in this article is to investigate the effect that the use of low-rank matrix approximation techniques to preprocess the data used as part of the model identification process would have on the performance of sparse model identification programs built over the basis of ideas used by Brunton, Kaheman, Kutz and Proctor in [6] and [17].

The main contribution of this article is the use of low-rank matrix approximation techniques to produce fast and easy to use sparse linear least squares solver algorithms, that can be effectively applied to sparse model identification processes. The low-rank approximation techniques that have been implemented provide a way to control the predictive model sensitivity to noise in the training data. As part of this research project, several general purpose computational tools for sparse model identification in science and engineering have been developed.

The constructive nature of the results presented in the sections §3 and §4 of this document allows one to derive prototypical algorithms like the ones presented in §5.1. Some numerical implementations of this prototypical algorithms based on Matlab, Python, Julia and Netgen/NGSolve are presented in §5.2.

2. PRELIMINARIES AND NOTATION

In this study, every time we refer to a system we will be considering a discrete-time dynamical system that can be described as a pair (Σ, \mathcal{T}) determined by a set of *states* $\Sigma \subset \mathbb{C}^n$, and a function $\mathcal{T} : \Sigma \rightarrow \Sigma$ that will be called a transition operator, such that for any time series determined by a sequence $\{x_t\}_{t \geq 1} \subset \Sigma$, we will have that $\mathcal{T}(x_t) = x_{t+1}$. For systems whose state spaces are contained in \mathbb{R}^n we will consider the usual identification of \mathbb{R} with the real line in \mathbb{C} , and will apply the system identification techniques presented in this study, considering suitable restrictions when necessary.

We will write \mathbb{Z}^+ to denote the set of positive integers $\mathbb{Z} \cap [1, \infty)$.

Given a set S , we will write $\sharp(S)$ to denote the number of elements in S .

In this document the symbol $\mathbb{C}^{n \times m}$ will denote the algebra of $n \times m$ complex matrices, and we will write I_n to denote the identity matrix in $\mathbb{C}^{n \times n}$ and $\mathbf{0}_{n,m}$ to denote the zero matrix in $\mathbb{C}^{n \times m}$, when $m = n$ we will write $\mathbf{0}_n$ instead of $\mathbf{0}_{n,n}$. From here on, given a matrix $X = [X_{ij}] \in \mathbb{C}^{m \times n}$, we will write X^* to denote the conjugate transpose of X determined by $X^* = \overline{X}^\top = [\overline{X}_{ji}]$ in $\mathbb{C}^{n \times m}$. We will represent vectors in \mathbb{C}^n as column matrices in $\mathbb{C}^{n \times 1}$ and as n -tuples.

Given any matrix $A \in \mathbb{C}^{m \times n}$ we will write $\text{rk}(A)$ to denote the rank of A , that corresponds to the maximal number of linearly independent columns of A .

Given $x \in \mathbb{C}^n$ we will write $\|x\|$ to denote the ℓ_2 -norm in \mathbb{C}^n determined by $\|x\| = \sqrt{x^*x} = (\sum_{j=1}^n |x_j|^2)^{1/2}$, and we will write $\|x\|_\infty$ to denote the ℓ_∞ -norm in \mathbb{C}^n determined by the expression $\|x\|_\infty = \max_{1 \leq j \leq n} |x_j|$ for each $x \in \mathbb{C}^n$.

In this document we will write $\hat{e}_{j,n}$ to denote the matrices in $\mathbb{C}^{n \times 1}$ representing the canonical basis of \mathbb{C}^n (each $\hat{e}_{j,n}$ is the j -column of I_n), that are determined by the expressions

$$(1) \quad \hat{e}_{j,n} = [\delta_{1,j} \quad \delta_{2,j} \quad \cdots \quad \delta_{n-1,j} \quad \delta_{n,j}]^\top$$

for each $1 \leq j \leq n$, where $\delta_{k,j}$ is the Kronecker delta determined by the expression.

$$(2) \quad \delta_{k,j} = \begin{cases} 1, & k = j \\ 0, & k \neq j \end{cases}$$

A matrix $P \in \mathbb{C}^{n \times n}$ will be called an orthogonal projector whenever $P^2 = P = P^*$. A matrix $Q \in \mathbb{C}^{m \times n}$ such that the matrices QQ^* and Q^*Q are orthogonal projectors will be called a partial isometry. We will write $\mathbb{U}(n)$ to denote the group of unitary matrices in $\mathbb{C}^{n \times n}$ defined by the expression $\mathbb{U}(n) = \{X \in \mathbb{C}^{n \times n} : X^*X = XX^* = I_n\}$.

Given $X = [x_{jk}] \in \mathbb{C}^{m \times n}$ and $Y = [y_{pq}] \in \mathbb{C}^{r \times s}$, we will write $X \otimes Y$ to denote the Kronecker product defined by the expression $X \otimes Y = [x_{jk}y_{pq}] \in \mathbb{C}^{(mr) \times (ns)}$.

Given $X \in \mathbb{C}^{n \times m}$ we will write $\|X\|_F$ to denote the Frobenius norm of X defined by

$$(3) \quad \|X\|_F = \sqrt{\text{tr}(X^*X)}$$

where tr denotes the trace of a matrix, defined for any $A = [a_{jk}] \in \mathbb{C}^{n \times n}$ by the expression.

$$\text{tr}(A) = \sum_{j=1}^n a_{jj}$$

Given a finite set of vectors $\Sigma_T = \{x_1, \dots, x_T\} \subset \mathbb{C}^n$ we will write $\mathcal{H}_L(\Sigma_T)$ to denote the Hankel-type trajectory matrix in $\mathbb{C}^{nL \times (T-L+1)}$ defined by the following expression.

$$\mathcal{H}_L(\Sigma_T) = \begin{bmatrix} x_1 & x_2 & x_3 & \cdots & x_{T-L+1} \\ x_2 & x_3 & x_4 & \cdots & x_{T-L+2} \\ x_3 & x_4 & x_5 & \cdots & x_{T-L+3} \\ \vdots & \vdots & \vdots & \cdots & \vdots \\ x_L & x_{L+1} & x_{L+2} & \cdots & x_T \end{bmatrix}$$

Given $a \in \mathbb{R}$, we will write H_a to denote the function $H_a : \mathbb{R} \rightarrow \mathbb{R}$ defined by the following expression.

$$(4) \quad H_a(x) = \begin{cases} 1, & x > a \\ 0, & x \leq a \end{cases}$$

For any additional details on the notions previously considered, the reader is kindly referred to [16], [1] and [15].

3. LOW-RANK APPROXIMATION AND SPARSE LINEAR LEAST SQUARES SOLVERS

In this section some low-rank approximation methods with applications to the solution of sparse linear least squares problems are presented.

Definition 3.1. Given $\delta > 0$ and a matrix $A \in \mathbb{C}^{m \times n}$, we will write $\text{rk}_\delta(A)$ to denote the nonnegative integer determined by the expression

$$\text{rk}_\delta(A) = \sum_{j=1}^{\min\{m,n\}} H_\delta(s_j(A)),$$

where the numbers $s_j(A)$ represent the singular values corresponding to an economy-sized singular value decomposition of the matrix A .

Lemma 3.2. *We will have that $\text{rk}_\delta(A^\top) = \text{rk}_\delta(A)$ for each $\delta > 0$ and each $A \in \mathbb{C}^{m \times n}$.*

Proof. Given an economy-sized singular value decomposition

$$U \begin{bmatrix} s_1(A) & & & \\ & s_2(A) & & \\ & & \ddots & \\ & & & s_{\min\{m,n\}}(A) \end{bmatrix} V = A$$

we will have that

$$V^\top \begin{bmatrix} s_1(A) & & & \\ & s_2(A) & & \\ & & \ddots & \\ & & & s_{\min\{m,n\}}(A) \end{bmatrix} U^\top = A^\top$$

is an economy-sized singular value decomposition of A^\top . This implies that

$$\text{rk}_\delta(A^\top) = \sum_{j=1}^{\min\{m,n\}} H_\delta(s_j(A)) = \text{rk}_\delta(A)$$

and this completes the proof. \square

Lemma 3.3. *Given $\delta > 0$ and $A \in \mathbb{C}^{m \times n}$ we will have that $\text{rk}_\delta(A) \leq \text{rk}(A)$.*

Proof. We will have that $\text{rk}(A) = \sum_{j=1}^{\min\{m,n\}} H_0(s_j(A)) \geq \sum_{j=1}^{\min\{m,n\}} H_\delta(s_j(A)) = \text{rk}_\delta(A)$. This completes the proof. \square

Theorem 3.4. *Given $\delta > 0$ and $y, x_1, \dots, x_m \in \mathbb{C}^n$, let*

$$X = \begin{bmatrix} | & | & \cdots & | \\ x_1 & x_2 & \cdots & x_m \\ | & | & \cdots & | \end{bmatrix}.$$

If $\text{rk}_\delta(X) > 0$ and if we set $r = \text{rk}_\delta(X)$ and $s_{n,m}(r) = \sqrt{r(\min\{m,n\} - r)}$ then, there are a rank r orthogonal projector Q , r vectors $x_{j_1}, \dots, x_{j_r} \in \{x_1, \dots, x_m\}$ and r scalars $c_1, \dots, c_r \in \mathbb{C}$ such that $\|X - QX\|_F \leq (s_{n,m}(r)/\sqrt{r})\delta$, and $\|y - \sum_{k=1}^r c_k x_{j_k}\| \leq (\sum_{k=1}^r |c_k|^2)^{\frac{1}{2}} s_{n,m}(r)\delta + \|(I_n - Q)y\|$.

Proof. Let us consider an economy-sized singular value decomposition $USV = A$. If u_j denotes the j -column of U , let Q be the rank $r = \text{rk}_\delta(A)$ orthogonal projector determined by the expression $Q = \sum_{j=1}^r u_j u_j^*$. It can be seen that

$$\begin{aligned} \|X - QX\|_F^2 &= \sum_{j=r+1}^{\min\{m,n\}} s_j(X)^2 \\ &\leq (\min\{m,n\} - r)\delta^2 = \frac{s_{n,m}(r)^2}{r}\delta^2. \end{aligned}$$

Consequently, $\|X - QX\|_F \leq \frac{s_{n,m}(r)}{\sqrt{r}}\delta$.

Let us set.

$$\begin{aligned} \hat{X} &= \begin{bmatrix} | & | & \cdots & | \\ \hat{x}_1 & \hat{x}_2 & \cdots & \hat{x}_m \\ | & | & \cdots & | \end{bmatrix} = QX \\ \hat{X}_y &= \begin{bmatrix} | & | & \cdots & | & | \\ \hat{x}_1 & \hat{x}_2 & \cdots & \hat{x}_m & \hat{y} \\ | & | & \cdots & | & | \end{bmatrix} = Q[X \quad y] \end{aligned}$$

Since by lemma 3.3 $\text{rk}(X) \geq \text{rk}_\delta(X)$, we will have that $\text{rk}(\hat{X}) = r = \text{rk}_\delta(X) > 0$, and since we also have that $\hat{x}_1, \dots, \hat{x}_m, \hat{y} \in \text{span}(\{u_1, \dots, u_r\})$, there are r linearly independent $\hat{x}_{j_1}, \dots, \hat{x}_{j_r} \in \{\hat{x}_1, \dots, \hat{x}_m\}$ such that $\text{span}(\{u_1, \dots, u_r\}) = \text{span}(\{\hat{x}_{j_1}, \dots, \hat{x}_{j_r}\})$, this in turn implies that $\hat{y} \in \text{span}(\{\hat{x}_{j_1}, \dots, \hat{x}_{j_r}\})$ and there are $c_1, \dots, c_r \in \mathbb{C}$ such that $\hat{y} = \sum_{k=1}^r c_k \hat{x}_{j_k}$. It can be seen that for each $z \in \{x_1, \dots, x_m\}$

$$\|z - Qz\| \leq \|X - QX\|_F \leq \frac{s_{n,m}(r)}{\sqrt{r}}\delta,$$

and this in turn implies that

$$\begin{aligned} \left\| y - \sum_{k=1}^r c_k x_{j_k} \right\| &= \left\| y - \sum_{k=1}^r c_k x_{j_k} - \left(\hat{y} - \sum_{k=1}^r c_k \hat{x}_{j_k} \right) \right\| \\ &= \left\| y - \sum_{k=1}^r c_k x_{j_k} - Q \left(y - \sum_{k=1}^r c_k x_{j_k} \right) \right\| \\ &\leq \left(\sum_{k=1}^r |c_k|^2 \right)^{\frac{1}{2}} s_{n,m}(r)\delta + \|(I_n - Q)y\|. \end{aligned}$$

This completes the proof. \square

As a direct implication of theorem 3.4 one can obtain the following corollary.

Corollary 3.5. *Given $\delta > 0$, $A \in \mathbb{C}^{m \times n}$ and $y \in \mathbb{C}^m$. If $\text{rk}_\delta(A) > 0$ and if we set $r = \text{rk}_\delta(A)$ and $s_{n,m}(r) = \sqrt{r(\min\{m, n\} - r)}$ then, there are $x \in \mathbb{C}^n$ and a rank r orthogonal projector Q that does not depend on y , such that $\|Ax - y\| \leq \|x\|s_{n,m}(r)\delta + \|(I_m - Q)y\|$ and x has at most r nonzero entries.*

Proof. Let us set $x = \mathbf{0}_{n,1}$ and $a_j = A\hat{e}_{j,n}$ for $j = 1, \dots, n$. Since $r = \text{rk}_\delta(A) > 0$ and $s_{n,m}(r) = \sqrt{r(\min\{m, n\} - r)}$, by theorem 3.4 we will have that there is a rank r orthogonal projector Q such that $\|A - QA\|_F \leq (s_{n,m}(r)/\sqrt{r})\delta$, and without loss of generality r vectors $a_{j_1}, \dots, a_{j_r} \in \{a_1, \dots, a_n\}$ and r scalars $c_1, \dots, c_r \in \mathbb{C}$ with $j_1 \leq j_2 \leq \dots \leq j_r$ (reordering the indices j_k if necessary), such that $\|y - \sum_{k=1}^r c_k a_{j_k}\| \leq \left(\sum_{k=1}^r |c_k|^2 \right)^{\frac{1}{2}} s_{n,m}(r)\delta + \|(I_m - Q)y\|$. If we set $x_{j_k} = c_k$ for $k = 1, \dots, r$, we will have that $\|x\| = \left(\sum_{k=1}^r |c_k|^2 \right)^{\frac{1}{2}}$ and $Ax = \sum_{k=1}^r x_{j_k} a_{j_k} = \sum_{k=1}^r c_k a_{j_k}$. Consequently, $\|Ax - y\| \leq \|x\|s_{n,m}(r)\delta + \|(I_m - Q)y\|$. This completes the proof. \square

Given $\delta > 0$, and two matrices $A \in \mathbb{C}^{m \times n}$ and $Y \in \mathbb{C}^{m \times p}$, we will write $AX \approx_\delta Y$ to represent the problem of finding $X \in \mathbb{C}^{n \times p}$, $\alpha, \beta \geq 0$ and an orthogonal projector Q such that $\|AX - Y\|_F \leq \alpha\delta + \beta\|(I_m - Q)Y\|_F$. The matrix X will be called a solution to the problem $AX \approx_\delta Y$.

Theorem 3.6. *Given $\delta > 0$, and two matrices $A \in \mathbb{C}^{m \times n}$ and $Y \in \mathbb{C}^{m \times p}$. If $\text{rk}_\delta(A) > 0$ and if we set $r = \text{rk}_\delta(A)$ then, there is a solution X to the problem $AX \approx_\delta Y$ with at most rp nonzero entries.*

Proof. Since $r = \text{rk}_\delta(A) > 0$ we can apply corollary 3.5 to each subproblem $Ax_j \approx_\delta Y\hat{e}_{j,p}$, to obtain p solutions x_1, \dots, x_p and a rank r orthogonal projector Q such that $\|Ax_j - Y\hat{e}_{j,p}\| \leq \|x_j\|s_{n,m}(r)\delta + \|(I_m - Q)Y\hat{e}_{j,p}\|$ for each $j = 1, \dots, p$ with $s_{n,m}(r) = \sqrt{r(\min\{m, n\} - r)}$, and each x_j has at most r nonzero entries. Consequently, if we set

$$X = \begin{bmatrix} | & & | \\ x_1 & \cdots & x_p \\ | & & | \end{bmatrix}$$

we will have that

$$\begin{aligned}
\|AX - Y\|_F^2 &= \sum_{j=1}^p \|Ax_j - Y\hat{e}_{j,p}\|^2 \\
&\leq \sum_{j=1}^p (\|x_j\|s_{n,m}(r)\delta + \|(I_m - Q)Y\hat{e}_{j,p}\|)^2 \\
&\leq \sum_{j=1}^p (\|X\|_F s_{n,m}(r)\delta + \|(I_m - Q)Y\|_F)^2 \\
&= p(\|X\|_F s_{n,m}(r)\delta + \|(I_m - Q)Y\|_F)^2
\end{aligned}$$

and this in turn implies that if we set $\alpha = \sqrt{p}s_{n,m}(r)\|X\|_F$ and $\beta = \sqrt{p}$, then

$$\|AX - Y\|_F \leq \alpha\delta + \beta\|(I_m - Q)Y\|_F.$$

Therefore, X is a solution to $AX \approx_\delta Y$ with at most rp nonzero entries. This completes the proof. \square

Although the sparse linear least squares solver algorithms and theoretical results in this article build on similar principles to the ones considered by Boutsidis and Magdon-Ismaïl in [3] and by Brunton, Proctor, and Kutz in [6]. One of the main differences of the approach considered in this study with the approach used in [3], is that given a least squares linear matrix equation $X = \arg \min_Y \|AY - B\|_F$, eventhough the rank $\text{rk}_\delta(A)$ approximation $A_\delta = QA$ corresponding to the matrix of coefficients A , is computed in a generic way using the orthogonal projector Q determined by theorem 3.4 and corollary 3.5 that in turn can be computed using a truncated economy-sized singular value decomposition of A with approximation error $\varepsilon = \mathcal{O}(\delta) > 0$, the selection process of each ordered set of the columns of A_δ corresponding to each column of the sparse approximate representation \hat{X} of the reference least squares solution X , is not random but B -dependent. And the main difference between the approach implemented in this study and the one implemented in [6], is that the sparse approximation process used here is based on reference solutions of least squares problems that involve submatrices of the low-rank approximation A_δ of the matrix of coefficients A instead of submatrices of the original matrix A .

More specifically, if A has n columns, once the low-rank approximation A_δ of A is computed along the lines of theorem 3.4, corollary 3.5 and theorem 3.6, for each column x_j of an initial reference least squares solution X of the problem $X = \arg \min_Y \|A_\delta Y - B\|_F$, one can set a threshold $\varepsilon > 0$, find an integer $N_j(\varepsilon) \leq \text{rk}_\delta(A)$ and compute a permutation $\sigma_j : \{1, \dots, n\} \rightarrow \{1, \dots, n\}$ based on the moduli $|x_{i,j}|$ of the entries of x_j according to the following conditions

$$\begin{aligned}
|x_{\sigma_j(1),j}| &\geq |x_{\sigma_j(2),j}| \geq \dots \geq |x_{\sigma_j(N_j(\varepsilon)),j}| > \varepsilon, \\
\varepsilon &\geq |x_{\sigma_j(N_j(\varepsilon)+1),j}| \geq \dots \geq |x_{\sigma_j(n-1),j}| \geq |x_{\sigma_j(n),j}|.
\end{aligned}$$

For each ordered subset $\hat{a}_{\sigma_j(1)}, \dots, \hat{a}_{\sigma_j(N_j(\varepsilon))}$ of columns of A_δ , we can solve the problems

$$\hat{x}_j = \arg \min_y \left\| \begin{bmatrix} | & & | \\ \hat{a}_{\sigma_j(1)} & \cdots & \hat{a}_{\sigma_j(N_j(\varepsilon))} \\ | & & | \end{bmatrix} y - b_j \right\|$$

for each $j = 1, \dots, p$.

If we define p vectors $\tilde{x}_1, \dots, \tilde{x}_p$ according to the following assignments

$$\tilde{x}_{\sigma_j(k),j} = \begin{cases} \hat{x}_{k,j}, & 1 \leq k \leq N_j(\varepsilon), \\ 0, & N_j(\varepsilon) < k \leq n \end{cases}$$

where $\tilde{x}_{i,j}$ and $\hat{x}_{k,j}$ denote the entries of each pair of vectors \tilde{x}_j and \hat{x}_j , respectively, we obtain a new approximate sparse solution

$$\tilde{X} = \begin{bmatrix} | & & | \\ \tilde{x}_1 & \cdots & \tilde{x}_p \\ | & & | \end{bmatrix}$$

to the problem $\hat{X} = \arg \min_Y \|A_\delta Y - B\|_F$. Using \tilde{X} as a new reference solution one can repeat this process for some prescribed number of times, or until some stopping criterion is met, in order to find a sparser representation of the initial reference solution X .

The results and ideas presented in this section can be translated into a sparse linear least squares solver algorithm described by algorithm 1 in §5.1.

4. LOW-RANK APPROXIMATION METHODS FOR SPARSE MODEL IDENTIFICATION

4.1. Sparse Identification of Transition Operators for Time Series with Symmetries. Given a sequence $\{x_t\}_{t \geq 1} \subset \mathbb{C}^n$, we say that $\{x_t\}_{t \geq 1}$ is a time series of a system (Σ, \mathcal{T}) , if $\{x_t\}_{t \geq 1} \subset \Sigma$ and $\mathcal{T}(x_t) = x_{t+1}$ for each $t \geq 1$. If in addition, there is a finite group $G_N = \{g_1, \dots, g_N\} \subset \mathbb{U}(n)$ such that

$$\mathcal{T}(g_j x_t) = g_j \mathcal{T}(x_t),$$

for each $t \geq 1$ and each $g_j \in G_N$, we will say that the system (Σ, \mathcal{T}) is G_N -equivariant and that the sequence $\{x_t\}_{t \geq 1}$ is a time series with symmetries.

We will say that a matrix $S \in \mathbb{C}^{n \times n}$ is symmetric with respect to a finite group $G_N = \{g_1, \dots, g_N\} \subset \mathbb{U}(n)$ if

$$g_j S = S g_j$$

for each $g_j \in G_N$. We will write $\mathbb{S}(n)^{G_N}$ to denote the set of all matrices in $\mathbb{C}^{n \times n}$ that are symmetric with respect to the group G_N .

Given an integer $L \geq 1$, a finite group $G_N \subset \mathbb{U}(n)$ with $\sharp(G_N) = N$, and a sample $\Sigma_T = \{x_t\}_{t=1}^T$ from a time series $\{x_t\}_{t \geq 1}$ in the state space $\Sigma \subset \mathbb{C}^n$ of some G_N -equivariant system (Σ, \mathcal{T}) , we will write $\mathcal{H}_L(\Sigma_T, G_N)$ to denote the structured block matrix with Hankel-type matrix blocks that is determined by the following expression.

$$\mathcal{H}_L(\Sigma_T, G_N) = \begin{bmatrix} (I_L \otimes g_1) \mathcal{H}_L(\Sigma_T) & \cdots & (I_L \otimes g_N) \mathcal{H}_L(\Sigma_T) \end{bmatrix}$$

Remark 4.1. *Since $G_N \subset \mathbb{U}(n)$ is a group, one of the elements in G_N is equal to I_n , consequently, one of the matrix blocks of $\mathcal{H}_L(\Sigma_T, G_N)$ is equal to $I_L \otimes I_n \mathcal{H}_L(\Sigma_T) = \mathcal{H}_L(\Sigma_T)$.*

Let us define the main sparse model identification problem for time series with symmetries.

Problem 1. Sparse model identification problem for time series with symmetries. *Given $\delta > 0$, an integer $L > 0$, a finite group $G_N \subset \mathbb{U}(n)$ with $\sharp(G_N) = N$, and a sample $\Sigma_T = \{x_t\}_{t=1}^T$ from a time series $\{x_t\}_{t \geq 1} \subset \mathbb{C}^n$ of a G_N -equivariant system (Σ, \mathcal{T}) with transition operator \mathcal{T} to be identified. Let $\Sigma_0 = \{x_1, \dots, x_{T-1}\}$, $\Sigma_1 = \{x_2, \dots, x_T\}$, $\mathbf{H}_{L,k} = \mathcal{H}_L(\Sigma_k, G_N)$ for $k = 0, 1$ and $\tilde{G}_N = \{I_L \otimes g_j : g_j \in G_N\}$. Determine if it is possible to compute a sparse matrix \hat{A}_T , a matrix $A_T \in \mathbb{S}(nL)^{\tilde{G}_N}$, an orthogonal projector Q and three nonnegative numbers \mathbb{D}, \mathbb{E} and \mathbb{F} such that if we set*

$$\begin{aligned} \nu &= \mathbb{D}\delta + \sqrt{nL} \|\mathbf{H}_{L,1}(I_{N(T-L)} - Q)\|_F, \\ \varepsilon &= \mathbb{E}\delta + \mathbb{F} \|\mathbf{H}_{L,1}(I_{N(T-L)} - Q)\|_F, \end{aligned}$$

then

$$\begin{aligned}
& \|\mathbf{H}_{L,1} - \hat{A}_T \mathbf{H}_{L,0}\|_F \leq \nu, \\
& \left\| \mathcal{F}(x_t) - \mathcal{P}_L \hat{A}_T^t X_1 \right\| \leq \varepsilon, \\
& \left\| \mathcal{F}(g_j x_t) - \mathcal{P}_L \hat{A}_T^t (I_L \otimes g_j) X_1 \right\| \leq \varepsilon, \\
& \|\mathbf{H}_{L,1} - A_T \mathbf{H}_{L,0}\|_F \leq \nu, \\
& \left\| \mathcal{F}(x_t) - \mathcal{P}_L A_T^t X_1 \right\| \leq \varepsilon, \\
& \left\| \mathcal{F}(g_j x_t) - \mathcal{P}_L A_T^t (I_L \otimes g_j) X_1 \right\| \leq \varepsilon
\end{aligned}$$

for each $t = 1, \dots, T - L$ and each $g_j \in G_N$, with $\mathcal{P}_L = \hat{e}_{1,L}^\top \otimes I_n$ and $X_1 = [x_1 \ \dots \ x_L]^\top$.

Definition 4.2. We will write $\mathbf{SDSI}(\Sigma_T, G_N, L, \delta)$ to denote the set of 6-tuples of solutions $(\hat{A}_T, A_T, Q, \mathbb{D}, \mathbb{E}, \mathbb{F})$ to problem 1 based on data Σ_T, G_N, L, δ .

Theorem 4.3. Given $\delta > 0$, a finite group $G_N \subset \mathbb{U}(n)$ with $\sharp(G_N) = N$, and a sample $\Sigma_T = \{x_t\}_{t=1}^T$ from a time series $\{x_t\}_{t \geq 1} \subset \mathbb{C}^n$ of a G_N -equivariant system (Σ, \mathcal{F}) with transition operator \mathcal{F} to be identified. If there is an integer $L > 0$ such that $\text{rk}_\delta \left(\mathcal{H}_L \left(\{x_t\}_{t=1}^{T-1}, G_N \right) \right) > 0$ then, there is $(\hat{A}_T, A_T, Q, \mathbb{D}, \mathbb{E}, \mathbb{F}) \in \mathbf{SDSI}(\Sigma_T, G_N, L, \delta)$.

Proof. Let $\mathbf{H}_{L,k} = \mathcal{H}_L(\Sigma_k, G_N)$ for $k = 0, 1$, with each Σ_k defined as in problem 1, and let us write $h_{j,k}$ to denote the $n \times (N(T - L))$ submatrix corresponding to the j -row block of $\mathbf{H}_{L,k}$ for $k = 0, 1$. By definition of $\mathbf{H}_{L,k}$ we will have that.

$$(5) \quad h_{j,1} = h_{j+1,0}, \quad 1 \leq j \leq L - 1$$

Let $\Sigma_{T-1} = \{x_t\}_{t=1}^{T-1}$. It can be seen that $\mathcal{H}_L(\Sigma_{T-1}, G_N) = \mathbf{H}_{L,0}$ and this in turn implies that

$$(6) \quad \mathcal{H}_{L+1}(\Sigma_T, G_N) = \begin{bmatrix} \mathcal{H}_L(\Sigma_{T-1}, G_N) \\ h_{L,1} \end{bmatrix} = \begin{bmatrix} \mathbf{H}_{L,0} \\ h_{L,1} \end{bmatrix}.$$

Since $\text{rk}_\delta(\mathbf{H}_{L,0}) = \text{rk}_\delta(\mathcal{H}_L(\Sigma_{T-1}, G_N)) > 0$, by lemma 3.2 we will have that

$$(7) \quad \text{rk}_\delta \left(\mathbf{H}_{L,0}^\top \right) = \text{rk}_\delta(\mathbf{H}_{L,0}) > 0.$$

Let us set $r = \text{rk}_\delta(\mathbf{H}_{L,0})$, $\mathcal{C} = \sqrt{r(\min\{nL, N(T - L)\} - r)}$, and let us write $h_{j,k,1}$ to denote the k -row of the j -row block $h_{j,1}$ of $\mathbf{H}_{L,1}$ for $j = 1, \dots, L$ and $k = 1, \dots, n$. By (5) and (7), applying corollary 3.5 to each pair $\mathbf{H}_{L,0}^\top, h_{j,k,1}^\top$ we can compute an orthogonal projector \hat{Q} and a vector $a_{j,k,T} \in \mathbb{C}^{1 \times (N(T-L))}$ such that

$$\begin{aligned}
& \left\| \mathbf{H}_{L,0}^\top a_{j,k,T}^\top - h_{j,k,1}^\top \right\| \leq \mathcal{C} \left\| a_{j,k,T}^\top \right\| \delta \\
& \quad + \left\| (I_{N(T-L)} - \hat{Q}) h_{j,k,1}^\top \right\|
\end{aligned}$$

(8)

and $a_{j,k,T}$ has at most r nonzero entries for each $j = 1, \dots, L$ and each $k = 1, \dots, n$. Let us set

$$\begin{aligned}
\hat{A}_T &= [a_{1,1,T}^\top \ \dots \ a_{1,n,T}^\top \ \dots \ a_{L,1,T}^\top \ \dots \ a_{L,n,T}^\top]^\top, \\
Q &= \hat{Q}^\top
\end{aligned}$$

and for each $t = 1, \dots, T - L$ and each $g_j \in G_N$, let us set

$$\begin{aligned}
X_t &= [x_t^\top \ \dots \ x_{t+L-1}^\top]^\top \\
Y_{j,t} &= I_L \otimes g_j X_t.
\end{aligned}$$

It can be easily verified that Q is an orthogonal projector, and by (8) if we set $\mathbb{D} = \sqrt{nL} \|\hat{A}_T\|_F \mathcal{C}$ we will have that

$$(9) \quad \begin{aligned} \left\| \mathbf{H}_{L,1} - \hat{A}_T \mathbf{H}_{L,0} \right\|_F &\leq \mathbb{D} \delta + \sqrt{nL} \left\| \mathbf{H}_{L,1} (I_{N(T-L)} - \hat{Q}^\top) \right\|_F \\ &= \mathbb{D} \delta + \sqrt{nL} \left\| \mathbf{H}_{L,1} (I_{N(T-L)} - Q) \right\|_F. \end{aligned}$$

Let us set $\mathbb{E} = \mathbb{D} \left(\sum_{t=0}^{T-1} \|\hat{A}_T\|_F^t \right)$ and $\mathbb{F} = \sqrt{nL} \left(\sum_{t=0}^{T-1} \|\hat{A}_T\|_F^t \right)$, by (9) and remark 4.1 we will have that

$$\begin{aligned} \|X_{t+1} - \hat{A}_T X_t\| &\leq \left\| \mathbf{H}_{L,1} - \hat{A}_T \mathbf{H}_{L,0} \right\|_F, \\ &\leq \mathbb{D} \delta + \sqrt{nL} \left\| \mathbf{H}_{L,1} (I_{N(T-L)} - Q) \right\|_F \\ \|Y_{j,t+1} - \hat{A}_T Y_{j,t}\| &\leq \left\| \mathbf{H}_{L,1} - \hat{A}_T \mathbf{H}_{L,0} \right\|_F \\ &\leq \mathbb{D} \delta + \sqrt{nL} \left\| \mathbf{H}_{L,1} (I_{N(T-L)} - Q) \right\|_F \end{aligned}$$

and this implies that

$$(10) \quad \begin{aligned} \|X_{t+1} - \hat{A}_T^t X_1\| &\leq \|X_{t+1} - \hat{A}_T X_t\| + \|\hat{A}_T X_t - \hat{A}_T^t X_1\| \\ &\leq \mathbb{D} \delta + \sqrt{nL} \left\| \mathbf{H}_{L,1} (I_{N(T-L)} - Q) \right\|_F \\ &\quad + \|\hat{A}_T\|_F \|X_t - \hat{A}_T^{t-1} X_1\| \\ &\dots \leq \mathbb{E} \delta + \mathbb{F} \left\| \mathbf{H}_{L,1} (I_{N(T-L)} - Q) \right\|_F \end{aligned}$$

and

$$(11) \quad \begin{aligned} \|Y_{j,t+1} - \hat{A}_T^t Y_{j,1}\| &\leq \|Y_{j,t+1} - \hat{A}_T Y_{j,t}\| + \|\hat{A}_T Y_{j,t} - \hat{A}_T^t Y_{j,1}\| \\ &\leq \mathbb{D} \delta + \sqrt{nL} \left\| \mathbf{H}_{L,1} (I_{N(T-L)} - Q) \right\|_F \\ &\quad + \|\hat{A}_T\|_F \|Y_{j,t} - \hat{A}_T^{t-1} Y_{j,1}\| \\ &\dots \leq \mathbb{E} \delta + \mathbb{F} \left\| \mathbf{H}_{L,1} (I_{N(T-L)} - Q) \right\|_F. \end{aligned}$$

Let us set

$$A_T = \frac{1}{N} \sum_{j=1}^N (I_L \otimes g_j^*) \hat{A}_T (I_L \otimes g_j).$$

Since $G_N = \{g_1, \dots, g_N\}$ is a finite group of unitary matrices and $N = \sharp(G_N)$, we will have that for each $1 \leq j, k \leq N$, there is $1 \leq l \leq N$ such that

$$I_L \otimes g_j I_L \otimes g_k = I_L \otimes g_j g_k = I_L \otimes g_l$$

and by elementary group representation theory this implies that for each $1 \leq k \leq N$

$$(I_L \otimes g_k)^* A_T (I_L \otimes g_k) = I_L \otimes g_k^* A_T I_L \otimes g_k = A_T.$$

Consequently,

$$(12) \quad I_L \otimes g_k A_T = A_T I_L \otimes g_k$$

for each $g_k \in G_N$, and this implies that $A_T \in \mathbb{S}(nL)^{\tilde{G}_N}$ with \tilde{G}_N defined as in problem 1.

By definition of A_T we will have that

$$\begin{aligned}
\|A_T\|_F &= \left\| \frac{1}{N} \sum_{j=1}^N (I_L \otimes g_j^*) \hat{A}_T (I_L \otimes g_j) \right\|_F \\
(13) \quad &\leq \frac{1}{N} \sum_{j=1}^N \|\hat{A}_T\|_F = \|\hat{A}_T\|_F
\end{aligned}$$

By definition of $\mathbf{H}_{L,0}, \mathbf{H}_{L,1}$ and by (9) and (12) we will have that

$$\begin{aligned}
\|X_{t+1} - A_T X_t\| &= \left\| \sum_{j=1}^N \frac{1}{N} X_{t+1} - \frac{1}{N} \sum_{j=1}^N I_L \otimes g_j^* \hat{A}_T I_L \otimes g_j X_t \right\| \\
&\leq \frac{1}{N} \sum_{j=1}^N \left\| I_L \otimes g_j X_{t+1} - \hat{A}_T I_L \otimes g_j X_t \right\| \\
&\leq \frac{1}{N} \sum_{j=1}^N \left\| \mathbf{H}_{L,1} - \hat{A}_T \mathbf{H}_{L,0} \right\|_F \\
&= \left\| \mathbf{H}_{L,1} - \hat{A}_T \mathbf{H}_{L,0} \right\|_F \\
&\leq \mathbb{D}\delta + \sqrt{nL} \left\| \mathbf{H}_{L,1}(I_{N(T-L)} - Q) \right\|_F \\
\|Y_{j,t+1} - A_T Y_{j,t}\| &= \|I_L \otimes g_j X_{t+1} - A_T I_L \otimes g_j X_t\| \\
&= \|I_L \otimes g_j (X_{t+1} - A_T X_t)\| \\
&= \|X_{t+1} - A_T X_t\| \\
&\leq \mathbb{D}\delta + \sqrt{nL} \left\| \mathbf{H}_{L,1}(I_{N(T-L)} - Q) \right\|_F.
\end{aligned}$$

Consequently, by (13) we will have that

$$\begin{aligned}
\|X_{t+1} - A_T^t X_1\| &\leq \|X_{t+1} - A_T X_t\| + \|A_T X_t - A_T^t X_1\| \\
&\leq \mathbb{D}\delta + \sqrt{nL} \left\| \mathbf{H}_{L,1}(I_{N(T-L)} - Q) \right\|_F \\
&\quad + \|\hat{A}_T\|_F \|X_t - A_T^{t-1} X_1\| \\
(14) \quad &\cdots \leq \mathbb{E}\delta + \mathbb{F} \left\| \mathbf{H}_{L,1}(I_{N(T-L)} - Q) \right\|_F
\end{aligned}$$

and

$$\begin{aligned}
\|Y_{j,t+1} - A_T^t Y_{j,1}\| &\leq \|Y_{j,t+1} - A_T Y_{j,t}\| + \|A_T Y_{j,t} - A_T^t Y_{j,1}\| \\
&\leq \mathbb{D}\delta + \sqrt{nL} \left\| \mathbf{H}_{L,1}(I_{N(T-L)} - Q) \right\|_F \\
&\quad + \|\hat{A}_T\|_F \|Y_{j,t} - A_T^{t-1} Y_{j,1}\| \\
(15) \quad &\cdots \leq \mathbb{E}\delta + \mathbb{F} \left\| \mathbf{H}_{L,1}(I_{N(T-L)} - Q) \right\|_F.
\end{aligned}$$

Since $\mathcal{T}(x_t) = x_{t+1}$ and since it is clear that \mathcal{P}_L is a partial isometry that satisfies $x_t = \mathcal{P}_L X_t$ and $g_j x_t = \mathcal{P}_L I_L \otimes g_j X_t$ for each $t = 1, \dots, T-L$ and each $g_j \in G_N$, by (14) we will have that

$$\begin{aligned} \left\| \mathcal{T}(x_t) - \mathcal{P}_L \hat{A}_T^t X_1 \right\| &= \left\| \mathcal{P}_L (X_{t+1} - \hat{A}_T^t X_1) \right\| \\ &\leq \left\| X_{t+1} - \hat{A}_T^t X_1 \right\| \\ &\leq \mathbb{E}\delta + \mathbb{F} \left\| \mathbf{H}_{L,1}(I_{N(T-L)} - Q) \right\|_F, \\ \left\| \mathcal{T}(x_t) - \mathcal{P}_L A_T^t X_1 \right\| &= \left\| \mathcal{P}_L (X_{t+1} - A_T^t X_1) \right\| \\ &\leq \left\| X_{t+1} - A_T^t X_1 \right\| \\ &\leq \mathbb{E}\delta + \mathbb{F} \left\| \mathbf{H}_{L,1}(I_{N(T-L)} - Q) \right\|_F \end{aligned}$$

and by (15) we will also have that

$$\begin{aligned} \left\| \mathcal{T}(g_j x_t) - \mathcal{P}_L \hat{A}_T^t (I_L \otimes g_j) X_1 \right\| &= \left\| g_j \mathcal{T}(x_t) - \mathcal{P}_L \hat{A}_T^t Y_{j,1} \right\| \\ &= \left\| \mathcal{P}_L (Y_{j,t+1} - \hat{A}_T^t Y_{j,1}) \right\| \\ &\leq \left\| Y_{j,t+1} - \hat{A}_T^t Y_{j,1} \right\| \\ &\leq \mathbb{E}\delta \\ &\quad + \mathbb{F} \left\| \mathbf{H}_{L,1}(I_{N(T-L)} - Q) \right\|_F, \\ \left\| \mathcal{T}(g_j x_t) - \mathcal{P}_L A_T^t (I_L \otimes g_j) X_1 \right\| &= \left\| g_j \mathcal{T}(x_t) - \mathcal{P}_L A_T^t Y_{j,1} \right\| \\ &= \left\| \mathcal{P}_L (Y_{j,t+1} - A_T^t Y_{j,1}) \right\| \\ &\leq \left\| Y_{j,t+1} - A_T^t Y_{j,1} \right\| \\ &\leq \mathbb{E}\delta \\ &\quad + \mathbb{F} \left\| \mathbf{H}_{L,1}(I_{N(T-L)} - Q) \right\|_F. \end{aligned}$$

This completes the proof. \square

We can apply theorem 4.3 for sparse model identification, specially when a sparse predictive model $\hat{\mathcal{T}}$ for a time series $\{x_t\}_{t \geq 1}$ of a system (Σ, \mathcal{T}) can be estimated for some given time horizon $T > 0$, based on a relatively small sample $\Sigma_S = \{x_t\}_{t=1}^S \subset \{x_t\}_{t \geq 1}$ for some $S \ll T$. Important examples of systems that would satisfy the previous consideration are the periodic and eventually periodic systems, like the ones considered in [13] and [11], respectively.

4.1.1. *An intuitive topological approach to sparse identification of time series models.* Let us consider the following set.

Definition 4.4. Given $\delta > 0$, a finite group $G_N \subset \mathbb{U}(n)$ with $\sharp(G_N) = N$, and a sample $\Sigma_T = \{x_t\}_{t=1}^T$ from a time series $\{x_t\}_{t \geq 1} \subset \mathbb{C}^n$ of a G_N -equivariant system (Σ, \mathcal{T}) . We will write $\text{Gr}_{\delta, \Sigma_T}^{G_N}$ to denote the δ -approximate symmetric identification grading set of the sample Σ_T that will be defined by the following expression

$$(16) \quad \text{Gr}_{\delta, \Sigma_T}^{G_N} = \left\{ 1 \leq L \leq \left\lfloor \frac{T+1}{2} \right\rfloor \mid \begin{array}{l} \text{rk}_\delta(\mathbf{H}_T^{L+1}) = \text{rk}_\delta(\mathbf{H}_{T-1}^L), \\ \text{rk}_\delta(\mathbf{H}_{T-1}^L) > 0 \end{array} \right\}$$

with $\mathbf{H}_T^{L+1} = \mathcal{H}_{L+1}(\Sigma_T, G_N)$ and $\mathbf{H}_{T-1}^L = \mathcal{H}_L(\{x_t\}_{t=1}^{T-1}, G_N)$.

Let us now consider a nonnegative integer defined as follows.

Definition 4.5. Given $\delta > 0$, a finite group $G_N \subset \mathbb{U}(n)$ with $\sharp(G_N) = N$, and a sample $\Sigma_T = \{x_t\}_{t=1}^T$ from a time series $\{x_t\}_{t \geq 1} \subset \mathbb{C}^n$ of a G_N -equivariant system (Σ, \mathcal{T}) . We will write $\text{deg}_{\delta, G_N}(\Sigma_T)$ to

denote the δ -approximate symmetric identification degree of the sample Σ_T that will be defined by the following expression.

$$(17) \quad \text{deg}_{\delta, G_N}(\Sigma_T) = \begin{cases} \inf \text{Gr}_{\delta, \Sigma_T}^{G_N} & , \#(\text{Gr}_{\delta, \Sigma_T}^{G_N}) \neq 0 \\ 0 & , \#(\text{Gr}_{\delta, \Sigma_T}^{G_N}) = 0 \end{cases}$$

From a topological perspective the approximate symmetric identification degree provides a way to compute invariants that can be used to classify samples from time series data in terms of the models that are computable based on such samples. More specifically, given a finite group $G_N \subset \mathbb{U}(n)$ with $\#(G_N) = N$, and a sample $\Sigma_T = \{x_t\}_{t=1}^T$ from a time series $\{x_t\}_{t \geq 1} \subset \mathbb{C}^n$ of a G_N -equivariant system (Σ, \mathcal{F}) such that $\text{deg}_{\delta, G_N}(\Sigma_T) = L > 0$ for some $\delta > 0$, we will have that if we set $\Sigma_{T-1} = \{x_t\}_{t=1}^{T-1}$ then

$$(18) \quad \text{rk}_{\delta}(\mathcal{H}_{L+1}(\Sigma_T, G_N)) = \text{rk}_{\delta}(\mathcal{H}_L(\Sigma_{T-1}, G_N)) > 0.$$

By (18) and as a consequence of theorems 3.6, 4.3 and the ideas implemented in their proofs, we will have that there are orthogonal projectors P, Q such that

$$(19) \quad \text{rk}(P) = \text{rk}(Q) = \text{rk}_{\delta}(\mathcal{H}_L(\Sigma_{T-1}, G_N)) > 0$$

and

$$(20) \quad \begin{aligned} \|P\mathcal{H}_L(\Sigma_{T-1}, G_N)^{\top} - \mathcal{H}_L(\Sigma_{T-1}, G_N)^{\top}\|_F &\leq C_1\delta, \\ \|Q\mathcal{H}_{L+1}(\Sigma_T, G_N)^{\top} - \mathcal{H}_{L+1}(\Sigma_T, G_N)^{\top}\|_F &\leq C_2\delta, \end{aligned}$$

for some constants $C_1, C_2 \geq 0$. By (19) we will have that as a consequence of the Schur decomposition theorem, there are unitaries U_P, U_Q such that

$$U_P^* P U_P = U_Q Q U_Q^*$$

this in turn implies that

$$P = U_P U_Q Q (U_P U_Q)^*$$

and by elementary Lie group theory there is an analytic path of unitaries $U(s) = e^{s \log(U_P U_Q)}$ from the identity matrix $I_{N(T-L)} = U(0)$ to $U_P U_Q = e^{\log(U_P U_Q)} = U(1)$, and this implies that there is an analytic path of orthogonal projectors $Q(s) = U(s) Q U(s)^*$ from Q to P . Consequently, the orthogonal projectors P and Q are homotopic in the sense that there is a homotopy between the corresponding constant maps over P and Q , respectively. In addition, by (6) and (20) we will have that P and Q satisfy the following norm constraint.

$$\|(P - Q)\mathcal{H}_L(\Sigma_{T-1}, G_N)^{\top}\|_F \leq (C_1 + C_2)\delta$$

Based on the previous considerations, we can observe that the number $\text{drk}_{\delta, G_N}(\Sigma_T)$ defined by the expression

$$\text{drk}_{\delta, G_N}(\Sigma_T) = \text{rk}_{\delta}(\mathcal{H}_{L+1}(\Sigma_T, G_N)) - \text{rk}_{\delta}(\mathcal{H}_L(\Sigma_{T-1}, G_N))$$

provides a way of measuring potential obstructions for the computability of predictive models based on Σ_T that can reach a prediction error $\mathcal{O}(\delta)$, in the sense that it would be necessary for $\text{drk}_{\delta, G_N}(\Sigma_T)$ to be equal to zero in order for the topological obstruction to be removed. A more formal study of these potential topologically controlled obstructions together with their connections with potential model overfitting, will be further studied in future communications.

Example 1. As an example of the previous phenomena, let us consider a sample $\Sigma_{257} = \{s_k : 1 \leq k \leq 257\}$ from a discrete time scalar signal $S = \{s_k : k \in \mathbb{Z}^+\}$ with trivial symmetry group $G_1 = \{1\}$, that is determined for each $k \in \mathbb{Z}^+$ by the expression

$$s_k = \sum_{j=0}^{\infty} \min\{t_k - j, 1 - t_k + j\} (H_j(t_k) - H_{j+1}(t_k))$$

with $t_k = (k - 1)/32$. Let us add noise to the sample Σ_{257} using a sequence of normally distributed pseudorandom numbers $\mathbf{RN}_{257} = \{r_k : |r_k| = \mathcal{O}(1 \times 10^{-3}), 1 \leq k \leq 257\}$, obtaining a noisy version $\tilde{\Sigma}_{257} = \{s_k + r_k : 1 \leq k \leq 257\}$ of the original sample Σ_{257} .

Let us consider a subsample $\tilde{\Sigma}_{70} = \{s_k + r_k : 1 \leq k \leq 70\} \subset \tilde{\Sigma}_{257}$. Computing $\text{deg}_{\delta, G_1}(\tilde{\Sigma}_{70})$ with $\delta = 1 \times 10^{-2}$ with the Matlab program `deg.m` in [31] we obtain $\text{deg}_{\delta, G_1}(\tilde{\Sigma}_{70}) = 17$. We can now compute a predictive model

$$s_{k+1} = c_1 s_k + c_2 s_{k-1} + \dots + c_L s_{k-L+1} \approx \mathcal{P}_L A_T^k \begin{bmatrix} s_1 \\ s_2 \\ \vdots \\ s_L \end{bmatrix}$$

for $k \geq L = \text{deg}_{\delta, G_1}(\tilde{\Sigma}_{70}) = 17$, along the lines of the proof of theorem 4.3 obtaining the following model

$$s_{k+1} = 1.000036116667133s_k - 0.998153385290551s_{k-15} + 0.998115019553671s_{k-16}$$

for $k \geq 17$.

The identified signals for different values of the lag parameter L are shown in figure 1.

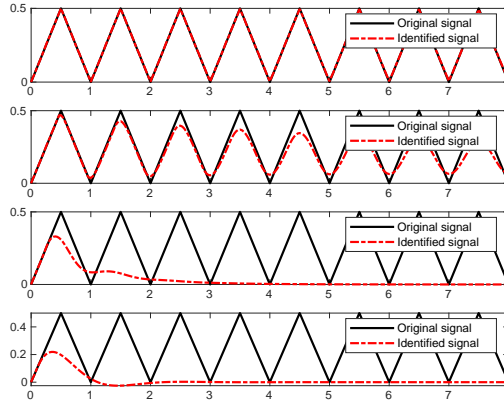


FIGURE 1. Identified signals for different lag values. $L = 17$ (top first row). $L = 16$ (second row). $L = 10$ (third row). $L = 5$ (bottom row).

The c_k coefficients corresponding to the models identified for different values of the lag parameter L are shown in figure 2. The root mean square error RMSE corresponding to different values of the lag parameter L are documented in table 1.

Lag value L	RMSE
17	0.002848195208845
16	0.067357195429571
10	0.265912048561782
5	0.279715847089058

TABLE 1. Root mean square errors corresponding to each lag value.

The computational setting used for this example is documented in the program `Example1.m` in [31]. For each lag value the corresponding model parameters were computed using program `SpSolver.m` in

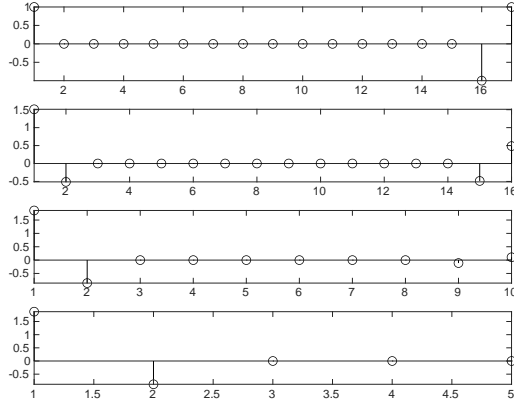


FIGURE 2. Identified coefficients for different lag values. $L = 17$ (top first row). $L = 16$ (second row). $L = 10$ (third row). $L = 5$ (bottom).

[31] based on algorithm 1, with the same tolerance $\delta > 0$, in order to expose the potential topologically controlled approximation obstruction identified by the number $\text{drk}_{\delta, G_1}(\tilde{\Sigma}_{70})$.

As a consequence of theorem 4.3 and the previous observations, it can be seen that given a finite group $G_N \subset \mathbb{U}(n)$ and a sample $\Sigma_T = \{x_t\}_{t=1}^T$ from a time series $\{x_t\}_{t \geq 1} \subset \mathbb{C}^n$ of a G_N -equivariant system (Σ, \mathcal{F}) , if the number $\hat{L} = \text{deg}_{\delta, G_N}(\Sigma_T)$ is positive, we can use this number to estimate a necessary condition for the computability of a sparse solution to the problem

$$\mathbf{H}_{L,0}^\top A_T^\top \approx_\delta \mathbf{H}_{L,1}^\top$$

where $\mathbf{H}_{L,k} = \mathcal{H}_L(\Sigma_k, G_N)$ for $k = 0, 1$, with $\Sigma_0 = \{x_t\}_{t=1}^{T-1}$ and $\Sigma_1 = \{x_t\}_{t=2}^T$. In particular, when $\hat{L} = \text{deg}_{\delta, G_N}(\Sigma_T)$ is positive, the lag value $L = \hat{L}$ would provide a good starting point for an adaptive sparse system identification method, if the prediction error is still not small enough for the lag value $L = \hat{L}$, a controlling algorithm can keep increasing the value of the lag parameter until the prediction error is reached or some prescribed bound for the lag value is attained. For the experiments documented in this article, we have used standard scalar signal autocorrelation techniques to estimate admissible bounds for the lag values, in the Sparse Dynamical System Identification (**SDSI**) toolset available in [31] these ideas are implemented in the Matlab program `LagEstimate.m` based on the Matlab function `xcorr.m`.

The results and ideas presented in this section can be translated into sparse identification algorithms like algorithm 2.

4.2. Sparse parameter identification for finite difference models. Let us write $\tilde{\partial}_{h,k}$ to denote the finite difference representation of the time differentiation operator ∂_t with approximation order k and uniform time partition size h . Given a dictionary of dynamic variables u_1, \dots, u_m , a function $f : (\mathbb{C}^n)^m \rightarrow (\mathbb{C}^n)^p$ and time series samples $\{u_j(k)\}_{k=1}^N \subset \mathbb{C}^n$ corresponding to each dynamic variable, let us write $V_N(f)(\mathbf{u})$ to denote the expression.

$$V_N(f)(\mathbf{u}) = \begin{bmatrix} f(u_1(1), \dots, u_m(1)) \\ \vdots \\ f(u_1(N), \dots, u_m(N)) \end{bmatrix}$$

In this section, given $\delta > 0$ we will consider the approximate sparse identification problems of the form

$$(21) \quad \begin{bmatrix} \hat{\mathfrak{D}}_{h,k}^1(\hat{u}_1) & \cdots & \hat{\mathfrak{D}}_{h,k}^m(\hat{u}_m) \end{bmatrix} \approx_{\delta} \begin{bmatrix} V_N(f_1)(\mathbf{u}) & \cdots & V_N(f_M)(\mathbf{u}) \end{bmatrix} \mathbf{C},$$

where $\hat{\mathfrak{D}}_{k,h}^1, \dots, \hat{\mathfrak{D}}_{k,h}^m$ denote finite difference operators based on $\mathfrak{D}_{k,h}$ with some additional specifications determined by the geometric or physical configuration of the system under study, and for each $1 \leq k \leq m$, $\hat{u}_k = V_N(p_k)(\mathbf{u})$ for p_k determined by the expression $p_k(x_1, \dots, x_m) = x_k$, and where each function $f_j : (\mathbb{C}^n)^{m_j} \rightarrow (\mathbb{C}^n)^{p_j}$ is given for $j = 1, \dots, M$.

By applying theorem 3.6 to (21) we obtain the following solvability result.

Corollary 4.6. *Given $\delta > 0$ and a problem of the form (21). If we set*

$$r = \text{rk}_{\delta} \left(\begin{bmatrix} V_N(f_1)(\mathbf{u}) & \cdots & V_N(f_M)(\mathbf{u}) \end{bmatrix} \right)$$

and if $r > 0$ then, there is a solution \mathbf{C} to the problem (21) with at most $r \sum_{k=1}^M p_k$ nonzero entries.

Proof. This is a direct application of theorem 3.6 to problem (21). □

Once an approximate sparse solution \mathbf{C} to the problem (21) has been computed, one can apply numerical time integration methods to the continuous-time approximate representation of (21) determined by the expression

$$\begin{bmatrix} \partial_t(\hat{u}_1) & \cdots & \partial_t(\hat{u}_m) \end{bmatrix} = \begin{bmatrix} f_1(\mathbf{u}) & \cdots & f_M(\mathbf{u}) \end{bmatrix} \mathbf{C},$$

with $f_j(\mathbf{u}) = f_j(u_1, \dots, u_m)$, in order to obtain a collection $\mathcal{T}_1, \dots, \mathcal{T}_m$ of transition operators that approximately satisfy the equations:

$$u_j(k+1) = \mathcal{T}_j(u_1(k), \dots, u_m(k))$$

for each $j = 1, \dots, m$, and each discrete time index $k \geq 1$.

5. COMPUTATIONAL METHODS

5.1. Algorithms. One of the purposes of this project is to provide sparse dynamical system identification (**SDSI**) tools that can be used to build collaborative frameworks of theoretical and computational methods that can be applied in a multidisciplinary context where adaptive approximate system identification is required. An example of the aforementioned collaborative frameworks can be described by the automaton illustrated in figure 3.

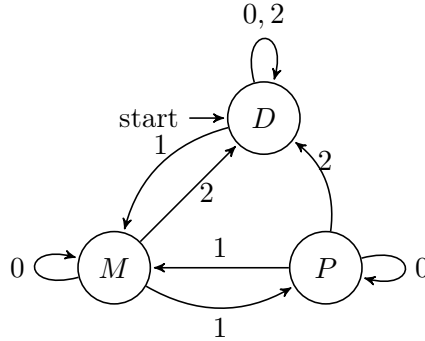


FIGURE 3. Finite-state automaton description of generic **SDSI** processes.

The blocks D , M and P of the system 3 correspond to the data processing, model computation and predictive simulation stages of a generic sparse system identification process, respectively, while the labels 0, 1 and 2 correspond to the states *computation in progress*, *computation completed* and *more data are required*, respectively.

In this document we focus on the sparse linear least squares solver algorithms and approximate topological invariants in the form of easily computable numbers, that can be used in the modeling block M of the automaton 3 for sparse model identification. Among other cases, the control signals for automata like 3 can be provided by an expert interested on the dynamics identification of some particular system, or by an artificially intelligent control system designed to build digital twins for a given system or process in some industrial environment. Although the programs in [31] can be used, adapted or modified to work in any of the two cases previously considered, the programs and examples included as part of the work reported in this document are written with the first case in mind. The artificially intelligent schemes will be further explored in the future.

Although the results in this document focus on sparse model identification, besides the programs corresponding to sparse linear least squares solvers and approximate degree and rank identifiers based on the results in §3 and §4, respectively, some programs for data reading and writing, synthetic signals generation, and predictive simulation are also include as part of the **SDSI** toolset available in [31].

5.1.1. *Sparse linear least squares solver algorithm.* As an application of the results and ideas presented in §3 one can obtain a prototypical sparse linear least squares solver algorithm like algorithm 1.

The least squares problems $c = \arg \min_{\hat{c} \in \mathbb{C}^K} \|\hat{A}\hat{c} - y\|$ to be solved as part of the process corresponding to algorithm 1 can be solved with any efficient least squares solver available in the language or program where the sparse linear least squares solver algorithm is implemented. For the Matlab and Julia implementations of algorithm 1 written as part of this research project the `backslash` "`\`" operator is used, and for the Python version of algorithm 1 the function `lstsq` is implemented.

5.1.2. *Sparse time series model identification algorithm.* Given a time series $\{x_t\}_{t \geq 1}$ of a system (Σ, \mathcal{T}) with transition operator \mathcal{T} to be identified, we can approach the computation of local approximations of \mathcal{T} based on a structured data sample $\Sigma_T = \{x_t\}_{t=1}^T \subset \Sigma$ using the prototypical algorithm outlined in algorithm 2.

For the study reported in this document, when the time series data $\Sigma_T = \{x_t\}_{t=1}^T \subset \mathbb{C}^n$ of a given system (Σ, \mathcal{T}) with transition operator \mathcal{T} to be identified, is not uniformly sampled in time, the sample Σ_T is preprocessed applying local spline interpolation methods to obtain a uniform in time estimate $\tilde{\Sigma}_T = \{\tilde{x}_t\}_{t=1}^T \subset \mathbb{C}^n$ for Σ_T . The Matlab program `DataSpliner.m` is an example of a computational implementation of this interpolation procedure and is included as part of the programs in the **SDSI** toolset available at [31].

Given a finite group $G_N \subset \mathbb{U}(n)$, a G_N -equivariant system (Σ, \mathcal{T}) and a structured data sample $\Sigma_T \subset \Sigma$, if the elements $\mathcal{P}, \hat{A}, A, X_1$ are computed using algorithm 2 with the setting $(\mathcal{P}, \hat{A}, A, X_1) = \mathbf{SDSI}(G_N, \tilde{\Sigma}_T, L, \delta, \varepsilon)$ for some suitable $\delta, \varepsilon > 0$, one can build two predictive models $\mathbf{P}_{\hat{A}}, \mathbf{P}_A$ for the time evolution of the system, determined by the recurrence relation $x_{t+1} = \mathcal{T}(x_t), t \geq 1$, using schemes of the form $\mathbf{P}_{\hat{A}}(t) = \mathcal{P}\hat{A}^t X_1$ and $\mathbf{P}_A(t) = \mathcal{P}A^t X_1$ for $t \geq 1$.

5.2. **Numerical Simulations.** In this section we will present some numerical simulations computed using the **SDSI** toolset available in [31], that was developed as part of this project, the toolset consists of a collection of programs written in Matlab, Julia and Python that can be used for sparse identification and numerical simulation of dynamical systems.

The numerical experiments documented in this section were performed with Matlab R2021a (9.10.0.1602886) 64-bit (glnxa64), Julia 1.6.0, Python 3.8 and Netgen/NGSolve 6.2. Some Matlab and Python Netgen/NGSolve programs were used to generate synthetic data used for some of the system identification processes. All the programs written for synthetic data generation and sparse model identification as part of this project are available at [31].

Algorithm 1 SLRSolver: Sparse linear least squares solver algorithm

Data: $A \in \mathbb{C}^{m \times n}$, $Y \in \mathbb{C}^{m \times p}$, $\delta > 0$, $N \in \mathbb{Z}^+$, $\varepsilon > 0$

Result: $X = \mathbf{SLRSolver}(A, Y, \delta, N, \varepsilon)$

- (1) Compute economy-sized SVD $USV = A$
- (2) Set $s = \min\{m, n\}$
- (3) Set $r = \text{rk}_\delta(A)$
- (4) Set $U_\delta = \sum_{j=1}^r U \hat{e}_{j,s} \hat{e}_{j,s}^*$
- (5) Set $T_\delta = \sum_{j=1}^r (\hat{e}_{j,s}^* S \hat{e}_{j,s})^{-1} \hat{e}_{j,s} \hat{e}_{j,s}^*$
- (6) Set $V_\delta = \sum_{j=1}^r \hat{e}_{j,s} \hat{e}_{j,s}^* V$
- (7) Set $\hat{A} = U_\delta^* A$
- (8) Set $\hat{Y} = U_\delta^* Y$
- (9) Set $X_0 = V_\delta^* T_\delta \hat{Y}$
- (10) **for** $j = 1, \dots, p$ **do**
 - Set $K = 1$
 - Set error = $1 + \delta$
 - Set $c = X_0 \hat{e}_{j,p}$
 - Set $x_0 = c$
 - Set $\hat{c} = [\hat{c}_1 \ \dots \ \hat{c}_n]^\top = [|\hat{e}_{1,n}^* c| \ \dots \ |\hat{e}_{n,n}^* c|]^\top$
 - Compute permutation $\sigma : \{1, \dots, n\} \rightarrow \{1, \dots, n\}$ such that: $\hat{c}_{\sigma(1)} \geq \hat{c}_{\sigma(2)} \geq \dots \geq \hat{c}_{\sigma(n)}$
 - Set $N_0 = \max \left\{ \sum_{j=1}^n H_\varepsilon(\hat{c}_{\sigma(j)}), 1 \right\}$
 - while** $K \leq N$ **and** error $> \delta$ **do**
 - Set $x = \mathbf{0}_{n,1}$
 - Set $A_0 = \sum_{j=1}^{N_0} \hat{A} \hat{e}_{\sigma(j),n} \hat{e}_{j,N_0}^*$
 - Solve $c = \arg \min_{\tilde{c} \in \mathbb{C}^{N_0}} \|A_0 \tilde{c} - \hat{Y} \hat{e}_{j,p}\|$
 - for** $k = 1, \dots, N_0$ **do**
 - Set $x_{\sigma(k)} = \hat{e}_{k,N_0}^* c$
 - end for**
 - Set error = $\|x - x_0\|_\infty$
 - Set $x_0 = x$
 - Set $\hat{c} = [\hat{c}_1 \ \dots \ \hat{c}_n]^\top = [|\hat{e}_{1,n}^* x| \ \dots \ |\hat{e}_{n,n}^* x|]^\top$
 - Compute permutation $\sigma : \{1, \dots, n\} \rightarrow \{1, \dots, n\}$ such that: $\hat{c}_{\sigma(1)} \geq \hat{c}_{\sigma(2)} \geq \dots \geq \hat{c}_{\sigma(n)}$
 - Set $N_0 = \max \left\{ \sum_{j=1}^n H_\varepsilon(\hat{c}_{\sigma(j)}), 1 \right\}$
 - Set $K = K + 1$
 - end while**
 - Set $x_j = x$
- (11) **end for**
- (12) Set $X = \begin{bmatrix} | & | & \dots & | \\ x_1 & x_2 & \dots & x_p \\ | & | & \dots & | \end{bmatrix}$

return X

The numerical simulations reported in this section were computed on a Linux Ubuntu Server 20.04 PC equipped with an Intel Xeon E3-1225 v5 (8M Cache, 3.30 GHz) processor and with 40GB RAM.

Algorithm 2 SDSI: algorithm for sparse dynamical system identification

Data: $G_N \subset \mathbb{U}(n)$, $\hat{\Sigma}_T = \{x_t\}_{t=1}^T \subset \mathbb{C}^n$, $L \in \mathbb{Z}^+$, $\delta > 0, \varepsilon > 0$

Result: $(\mathcal{P}_L, \hat{A}_T, A_T, X_1) = \text{SDSI}(G_N, \hat{\Sigma}_T, L, \delta, \varepsilon)$

- (1) Compute $L = \max\{\text{deg}_{\delta, G_N}(\hat{\Sigma}_T), L\}$
- (2) Set $\hat{\Sigma}_0 = \{x_t\}_{t=1}^{T-1}$, $\hat{\Sigma}_1 = \{x_t\}_{t=2}^T$
- (3) Set $\mathbf{H}_{L,k} = \mathcal{H}_L(\hat{\Sigma}_k, G_N)$, $k = 0, 1$
- (4) Solve $\mathbf{H}_{L,0}^\top C \approx_{\delta} \mathbf{H}_{L,1}^\top$ applying algorithm 1 with the setting $C = \text{SLRSolver}(\mathbf{H}_{L,0}^\top, \mathbf{H}_{L,1}^\top, \delta, nL, \varepsilon)$
- (5) Set $\hat{A}_T = C^\top$
- (6) Set $A_T = \frac{1}{N} \sum_{j=1}^N (I_L \otimes g_j^*) \hat{A}_T (I_L \otimes g_j)$
- (7) Set $X_1 = [x_1^\top \cdots x_L^\top]^\top$
- (8) Set $\mathcal{P}_L = \hat{e}_{1,L}^\top \otimes I_n$

return $(\mathcal{P}_L, \hat{A}_T, A_T, X_1)$

5.2.1. *Sparse identification of a finite difference model for the nonlinear Schrödinger equation in the finite line.* In this section a finite difference model corresponding to a nonlinear Schrödinger equation of the form

$$(22) \quad i\partial_t w + \partial_x^2 w + q|w|^2 w = 0$$

for $x \in [-20, 20]$ and $t \geq 0$, will be approximately identified. The synthetic signals corresponding to the csv data file `NLSEqData.csv` that will be used for system identification have been computed using a fourth order Runge-Kutta scheme to integrate the corresponding second order in space finite difference discretization of (22), with initial conditions and homogeneous Dirichlet boundary conditions based on the configuration used by Ramos and Villatoro in [24] using the Matlab program `NLSchrodinger1DRK.m` in [31]. The amplitudes corresponding to the dynamical behavior data $\Sigma_{4401} = \{\mathbf{w}(t)\}_{t=1}^{4401} \subset \mathbb{C}^{161}$ saved in file `NLSEqData.csv` are visualized in figure 4.

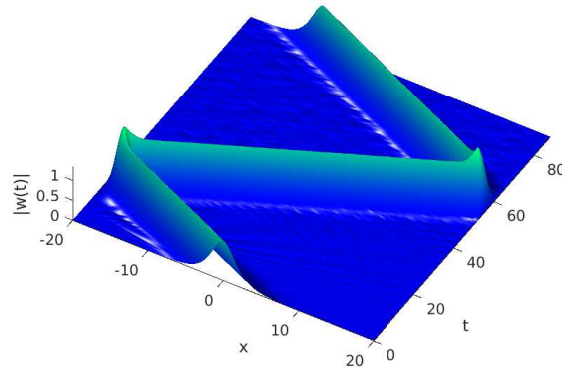


FIGURE 4. Amplitudes corresponding to an approximation of a travelling wave solution to equation (22).

Let us consider the finite difference model

$$(23) \quad i\hat{\mathcal{D}}_{h_t,4} \mathbf{w} + \mathbf{D}_{h_x,2} \mathbf{w} + q|\mathbf{w}|^2 \mathbf{w} = 0$$

corresponding to (22), where the operation $\hat{\partial}_{h_t,4}\mathbf{w}(t)$ is defined for an arbitrary differentiable function $t \mapsto \mathbf{w}(t) = [w_1(t) \ \cdots \ w_{161}(t)]^\top \in \mathbb{C}^{161}$ by the expression

$$\hat{\partial}_{h_t,4}\mathbf{w}(t) = [0 \ \partial_{h_t,4}w_2(t) \ \cdots \ \partial_{h_t,4}w_{160}(t) \ 0]^\top.$$

The choice of fourth order approximations $\partial_{h_t,4}w_k(t)$ of each derivative $\partial_t w_k(t)$ for $2 \leq k \leq 160$, is based on the fact that the synthetic data Σ_{4401} recorded in `NLSEqData.csv` were computed using a fourth order Runge-Kutta scheme for time integration.

We will apply algorithm 1 along the lines of corollary 4.6 to identify model (23), using a dictionary of 203 functions $f_j : \mathbb{C}^{161} \rightarrow \mathbb{C}^{161}$ defined in terms of a generic $\mathbf{u} = [u_j] \in \mathbb{C}^{161}$ by the following expressions

$$\begin{aligned} f_1(\mathbf{u}) &= [0 \ u_2 \ u_3 \ \cdots \ u_{160} \ 0]^\top, \\ f_2(\mathbf{u}) &= [0 \ 0 \ u_2 \ u_3 \ \cdots \ u_{159} \ 0]^\top \\ f_3(\mathbf{u}) &= [0 \ u_3 \ u_4 \ \cdots \ u_{160} \ 0 \ 0]^\top \\ f_4(\mathbf{u}) &= [0 \ |u_2|u_2 \ |u_3|u_3 \ \cdots \ |u_{160}|u_{160} \ 0]^\top, \\ f_5(\mathbf{u}) &= [0 \ |u_2|^2u_2 \ |u_3|^2u_3 \ \cdots \ |u_{160}|^2u_{160} \ 0]^\top, \\ &\vdots \\ f_{203}(\mathbf{u}) &= [0 \ |u_2|^{200}u_2 \ |u_3|^{200}u_3 \ \cdots \ |u_{160}|^{200}u_{160} \ 0]^\top. \end{aligned}$$

Since the synthetic data Σ_{4401} was generated using Runge-Kutta approximation of a second order finite difference discretization of (22), there is some numerical noise induced in the synthetic signal due to floating point errors, in addition, for this experiment some pseudorandom noise with $\mathcal{O}(10^{-6})$ is added to the reference data Σ_{4401} to obtain a noisier version $\tilde{\Sigma}_{4401}$ of Σ_{4401} that has been recorded in [31] as `NoisyNLSEqData.csv` for future references.

Some reference data corresponding to the amplitude $|w|$ of w together with the predictions computed with the model that has been identified using the sparse solver of the SDSI toolset are visualized in figure 5.

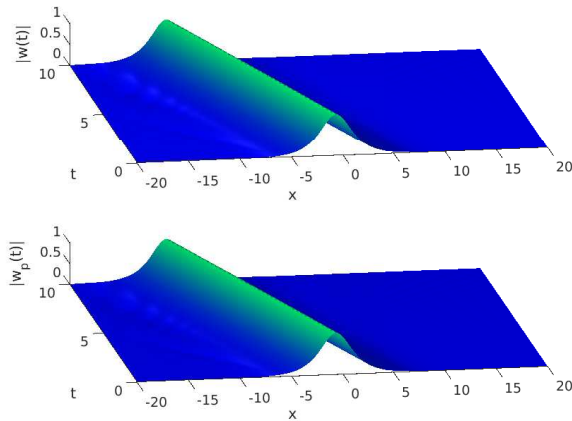
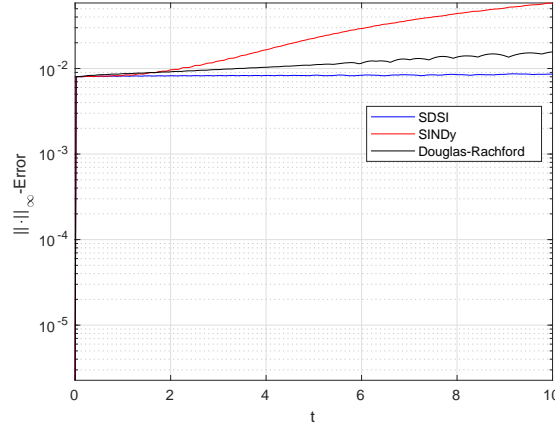


FIGURE 5. Reference data amplitudes $|w(t)|$ (top). Predicted values of the amplitudes $|w_p(t)|$ computed with SDSI model identifier (bottom).

The sparse identification of the signal data Σ_{4401} corresponding to the discretization (23) of (22) was also computed using standard SINDy and Douglas-Rachford sparse solvers as presented and implemented in [6] and [27]. The absolute prediction errors corresponding to the SDSI, SINDy and

FIGURE 6. Prediction errors in the ℓ_∞ -norm.

Douglas-Rachford solvers in the ℓ_∞ -norm are shown in figure 6. The running times are documented in the table 2.

Method	Running Time (seconds)
SDSI	0.122988
SINDy	0.258558
Douglas-Rachford	286.864170

TABLE 2. Running time of the sparse identification methods

Let us write w_k to denote the k -component of the state vector $\mathbf{w}(t) \in \mathbb{C}^{161}$ determined by the expression $w_k = w(-20 + (k-1)h_x, th)$ for $h_x = 1/4$ and $h = 1/10$. The corresponding semi-discrete model will be

$$i\dot{w}_k = -32w_k + 16w_{k+1} + 16w_{k-1} + |w_k|^2 w_k, 2 \leq k \leq 160$$

with $w_1 = w_{161} = 0$. The semi-discrete models identified by each method based on a training set of 35 samples $\tilde{\Sigma}_{35} = \{\tilde{\mathbf{w}}(1), \dots, \tilde{\mathbf{w}}(35)\} \subset \tilde{\Sigma}_{4401}$ for each $2 \leq k \leq 160$ are documented in table 3, for every model in the table $w_1 = w_{161} = 0$.

Method	Identified Model
SDSI	$i\dot{w}_k = (-31.8766 - 0.0276i)w_k + (15.9414 + 0.0211i)w_{k+1} + (15.9381 + 0.0059i)w_{k-1} + (0.9962 + 0.0008i) w_k ^2 w_k$
SINDy	$i\dot{w}_k = (-31.8705 - 0.0646i)w_k + (15.9408 + 0.0390i)w_{k+1} + (15.9330 + 0.0231i)w_{k-1} + (-0.0340 + 0.1333i) w_k w_k + (2.8996 - 6.5725i) w_k ^2 w_k + (-52.3400 + 160.4634i) w_k ^3 w_k + (790.9174 - 2.2437 \times 10^3) w_k ^4 w_k + (25 \text{ more terms})$
Douglas-Rachford	$i\dot{w}_k = (-29.0860 - 0.0599i)w_k + (14.5809 + 0.2070i)w_{k+1} + (14.5735 - 0.1480i)w_{k-1} + (0.9042 + 0.0012i) w_k ^2 w_k + (0.0045 - 0.0002i) w_k ^3 w_k$

TABLE 3. Model Identified by each method

The computational setting used for this experiment is documented in the Matlab program `NLSESpModelID.m` in [31] that can be used to replicate this experiment.

5.2.2. *Sparse identification of a network of Duffing oscillators with symmetries.* In this section a network of three coupled Duffing oscillators with the following configuration

$$\begin{aligned}
 \dot{x}_i &= y_i, \quad i \in \{1, 2, 3\} \\
 \dot{y}_i &= \sigma y_j - x_i(\beta + \alpha^2 x_i) + \sum_{ij} \eta_{ij}(x_i - x_j), \quad i \in \{1, 2, 3\} \\
 x_1(0) &= 8, x_2(0) = 7, x_3(0) = 4, \\
 y_1(0) &= 15, y_2(0) = 14, y_3(0) = 9
 \end{aligned}
 \tag{24}$$

is identified, for $\alpha = 1, \beta = -36, \sigma = 0$ and with all the coupling strengths η_{ij} equal to $1/5$. The configuration of these experiment is based on the example II.2 considered in [26], an important part of the motivation for the study of this types of networks of oscillators comes from interesting applications in engineering and biological cybernetics like the ones presented in [10], [25] and [9]. Since all the coupling strengths η_{ij} are equal to $1/5$, as established in [26] the system (24) will be D_3 -equivariant, and for the configuration used for this experiment, the matrix representation of the corresponding group of symmetries $D_3 = \langle r, \kappa | r^3 = \kappa^2 = e, \kappa r \kappa = r^{-1} \rangle$ is determined by the following assignments.

$$\begin{aligned}
 r \mapsto r_\rho &= I_2 \otimes \begin{bmatrix} 0 & 1 & 0 \\ 0 & 0 & 1 \\ 1 & 0 & 0 \end{bmatrix} \\
 \kappa \mapsto \kappa_\rho &= I_2 \otimes \begin{bmatrix} 1 & 0 & 0 \\ 0 & 0 & 1 \\ 0 & 1 & 0 \end{bmatrix}
 \end{aligned}$$

The synthetic signal used for sparse identification of (24) was computed with an adaptive fourth order Runge-Kutta scheme. The model was trained using the dictionary

$$\begin{aligned}
 f_1(x_1, x_2, x_3, y_1, y_2, y_3) &= (x_1, x_2, x_3, y_1, y_2, y_3) \\
 f_2(x_1, x_2, x_3, y_1, y_2, y_3) &= (x_1^2, x_2^2, x_3^2) \\
 f_3(x_1, x_2, x_3, y_1, y_2, y_3) &= (x_1^3, x_2^3, x_3^3) \\
 &\vdots \\
 f_9(x_1, x_2, x_3, y_1, y_2, y_3) &= (x_1^9, x_2^9, x_3^9)
 \end{aligned}$$

with 20% of the synthetic reference data.

The reference synthetic signal and the corresponding identified signals are illustrated in figure 7

The prediction errors $\|\mathbf{x}(t) - \mathbf{x}_p(t)\|$, and the equivariance errors $\|F(r_\rho \mathbf{x}(t)) - r_\rho F(\mathbf{x}(t))\|$ and $\|F(\kappa_\rho \mathbf{x}(t)) - \kappa_\rho F(\mathbf{x}(t))\|$ of the identified right hand side F for a model $\dot{x} = F(x)$ of the form (24), for each discrete time index t are plotted in figure 8.

The models identified by each method are documented in tables 4 and 5.

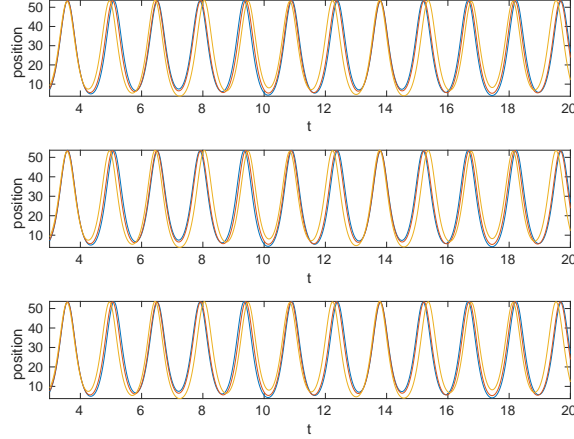


FIGURE 7. Synthetic reference position signals (top). Signals identified using SDSI sparse solver (middle). Signals identified using SINDy sparse solver (bottom).

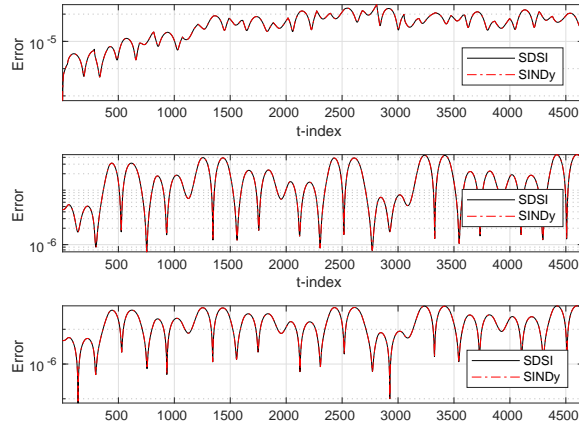


FIGURE 8. Prediction errors (top). Equivariance errors for r_ρ (middle). Equivariance errors for κ_ρ (bottom).

Method	Identified Model
SDSI	$\begin{aligned} \dot{x}_1 &= 0.999999992419860y_1, \\ \dot{x}_2 &= 0.999999992358200y_2, \\ \dot{x}_3 &= 0.999999992182884y_3, \\ \dot{y}_1 &= 36.399999678455494x_1 - 0.200001381665299x_2 - 0.199999513388808x_3 \\ &\quad - 0.9999999696376x_1^2, \\ \dot{y}_2 &= -0.199999469429072x_1 + 36.399998021632314x_2 - 0.199999719964769x_3 \\ &\quad - 0.999999971061446x_2^2, \\ \dot{y}_3 &= -0.199998908401240x_1 - 0.200001498693973x_2 + 36.399999282587004x_3 \\ &\quad - 0.999999971862063x_3^2, \end{aligned}$

TABLE 4. Model Identified by SDSI.

Method	Identified Model
SINDy	$\dot{x}_1 = 0.999999992419860y_1,$ $\dot{x}_2 = 0.999999992358200y_2,$ $\dot{x}_3 = 0.999999992182883y_3,$ $\dot{y}_1 = 36.399999678455423x_1 - 0.200001381665187x_2 - 0.199999513388848x_3$ $- 0.99999969696376x_1^2,$ $\dot{y}_2 = -0.199999469429017x_1 + 36.399998021632094x_2 - 0.199999719964673x_3$ $- 0.99999971061444x_2^2,$ $\dot{y}_3 = -0.199998908401247x_1 - 0.200001498693980x_2 + 36.399999282587018x_3$ $- 0.99999971862063x_3^2,$

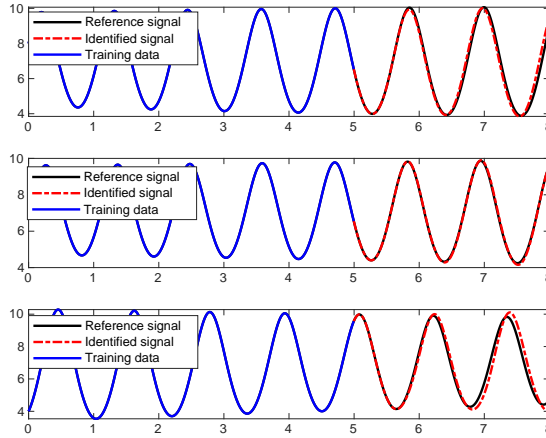
TABLE 5. Model Identified by SINDy.

The running times for the computation of each model are documented in table 6.

Method	Running Time (seconds)
SDSI	0.002407
SINDy	0.001376

TABLE 6. Running times for the computation of the nonlinear model identifications.

Using the same data we can apply algorithm 2 to compute a local linear model approximant for the model 24. The identified signals computed using SDSI sparse solver are shown in figure 9 and the identified signals computed using SINDy sparse solver are shown in figure 10.

FIGURE 9. Signal identification computed with SDSI for: x_1 (top). x_2 (middle). x_3 (bottom).

The sparsity patterns of the matrices of parameters identified by each method are shown in figure 11.

Let us set $\hat{r}_\rho = I_L \otimes r_\rho$ and $\hat{\kappa}_\rho = I_L \otimes \kappa_\rho$. The numerical errors corresponding to the symmetry constraints imposed to the matrices of parameters are documented in table 7.

Method	$\ \hat{r}_\rho A_T - A_T \hat{r}_\rho\ _F$	$\ \hat{\kappa}_\rho A_T - A_T \hat{\kappa}_\rho\ _F$
SDSI	$6.311151928321685 \times 10^{-16}$	0
SINDy	$9.138315630890346 \times 10^{-16}$	0

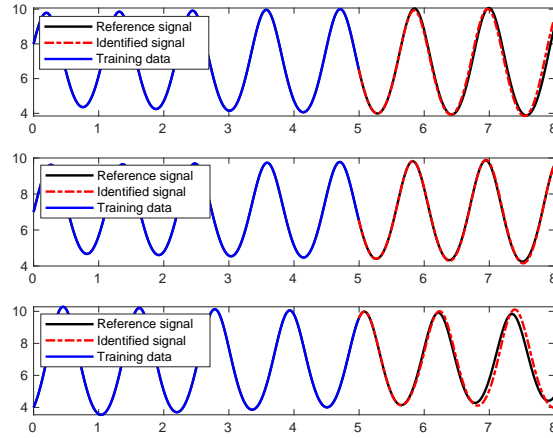


FIGURE 10. Signal identification computed with SINDy for: x_1 (top). x_2 (middle). x_3 (bottom).

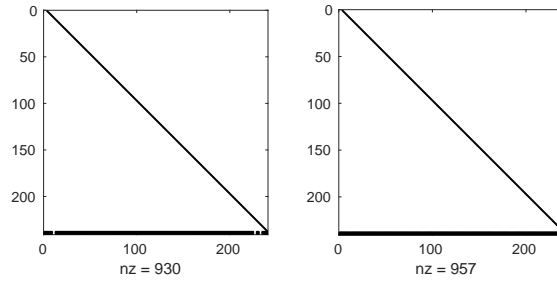


FIGURE 11. Sparsity pattern of the matrix of parameters identified by: SDSI (left). SINDy (right).

TABLE 7. Numerical errors corresponding to the symmetry preserving constraints.

The root mean square errors corresponding to the variables considered for the local linear model approximants are documented in table 8, and the running times corresponding to the computation of the local linear model approximants are documented in table 9.

Variable	RMSE (SDSI)	RMSE (SINDy)
x_1	0.153492169453791	0.154497134958370
x_2	0.032257712638561	0.032739961411393
x_3	0.227124393816712	0.227994328981342

TABLE 8. Root mean square errors corresponding to each method and variable.

Method	Running Time (seconds)
SDSI	0.095987
SINDy	0.420293

TABLE 9. Running times for the computation of the local linear model approximant.

The computational setting used for the experiments performed in this section is documented in the Matlab programs `NLONetworkID.m` and `DuffingLTIModelID.m` in [31] that can be used to replicate these experiments.

5.2.3. *Sparse identification of a time series model for vortex shedding processes.* Let us consider a Navier-Stokes nonlinear model of the form

$$(25) \quad \begin{aligned} \frac{\partial u}{\partial t} + u \cdot \nabla u - \nu \Delta u + \nabla p &= 0 \\ \nabla \cdot u &= 0 \end{aligned}$$

under suitable geometric configuration, initial and boundary conditions that lead to vortex shedding. For this experiment, the sparse model identification process is based on the synthetic data corresponding to a vortex shedding process recorded in the file `GFUdata.csv`, that is included in [31] as the compressed file `GFUdata.zip`, the synthetic data were generated using the program `navierstokes-tcsi.py` included in [31] that is based on the Netgen/Python program `navierstokes.py` developed by J. Schöberl as part of the work initiated with [29].

The time series model identification based on the data $\Sigma_{502} = \{u_t\}_{t=1}^{502} \subset \mathbb{R}^{53770}$ recorded in `GFUdata.csv` is performed with a computational implementation of algorithm 2 using the Matlab program `NSIdentifier.m` which estimates the number $\deg_{9 \times 10^{-7}, \{I_{53770}\}}(\Sigma_{400})$ obtaining the value $\deg_{9 \times 10^{-7}, \{I_{53770}\}}(\Sigma_{400}) = 1$, for this experiment we have that $\text{rk}_\delta(\mathcal{H}_1(\Sigma_{400})) = 354$, and the models are trained with the subsample $\Sigma_{354} = \{u_t\}_{t=1}^{354} \subset \Sigma_{400} \subset \Sigma_{502}$.

Since $d = 1$, the models can be computed using the reduced form

$$u_{k+1} = \mathcal{H}_1(\Sigma_{353}) A_{353}^k \hat{e}_{1,353}, \quad k \geq 1$$

with $\Sigma_{353} = \{u_t\}_{t=1}^{353}$, and only a matrix of parameters A_{353} is left to be identified. The matrix of parameters will be identified using the sparse solver `SpSolver.m` from the SDSI toolset based on algorithm 1 and the sparse solver `SINDy.m` based on SINDy sparse least squares solver algorithm introduced in [6].

The sparsity patterns of the matrices of parameters identified by the Matlab programs `SpSolver.m` and `SINDy.m` are shown in figure 12.

The reference state u_{502} and the corresponding states predicted by SINDy and SDSI algorithms are shown in figure 13.

The prediction error estimates $\|\mathcal{H}_1(\Sigma_{502}) - \mathcal{H}_1(\hat{\Sigma}_{502})\|_F$ for the predicted states $\hat{\Sigma}_{502}$ computed with each method are documented in table 10, and the running times corresponding to the computation of the sparse representations of the matrices of parameters are documented in table 11.

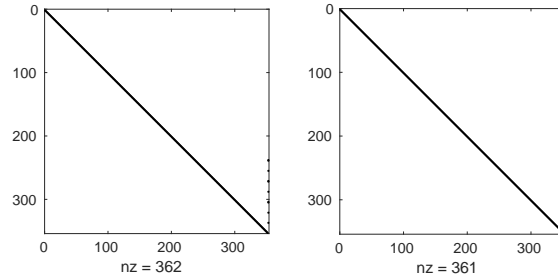


FIGURE 12. Sparsity patterns of matrices of parameters identified by: SINDy solver (left) and SDSI solver (right).

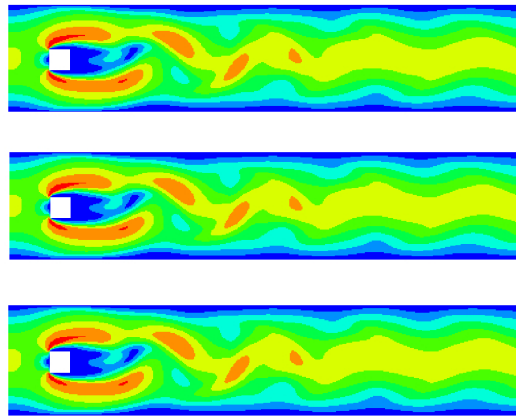


FIGURE 13. Reference u_{502} state (top). Predicted \hat{u}_{502} state with SDSI (middle). Predicted \hat{u}_{502} state with SINDy (bottom).

Method	$\ \mathcal{H}_1(\Sigma_{502}) - \mathcal{H}_1(\hat{\Sigma}_{502})\ _F$
SDSI	0.0057
SINDy	0.0072

TABLE 10. Prediction error estimates corresponding to each method.

Method	Running Time (seconds)
SDSI	1.371872
SINDy	6.017688

TABLE 11. Running times for the computation of the local linear model approximant.

The computational setting used for this experiment is documented in the Matlab script `NSIdentifier.m` in [31]. There are also Julia and Python versions of this script included in [31], but only the Matlab version was documented in this article as it is the fastest version of the algorithm 2,

probably due in part to the outstanding performance of the least squares solver implemented in Matlab via the "\ " operator.

5.2.4. *Sparse identification of a weather forecasting model.* For this example we will use a subcollection of the weather time series dataset recorded by the Max Planck Institute for Biogeochemistry, that was collected between 2009 and 2016 and prepared by François Chollet for [8]. From the column T (degC) of the corresponding table, a subsample $\Sigma_{8412} \subset \mathbb{R}$ uniformly sampled in time with 8412 elements has been extracted and recorded as `TemperatureData.csv` for future references as part of [31].

Using 50% of the data in Σ_{8412} we can compute three weather forecasting models of the form

$$T_{k+1} = c_0 + c_1 T_k + c_2 T_{k-1} + \cdots + c_L T_{k-L+1}$$

$$\approx c_0 + \mathcal{P}_L A_T^k \begin{bmatrix} T_1 \\ T_2 \\ \vdots \\ T_L \end{bmatrix}.$$

The first model will be computed using the function `AutoReg` from the module `statsmodels` from Python, the second model will be computed applying algorithm 2 with the sparse solver `SINDy.m`, and the third model will be computed applying algorithm 2 with the sparse solver `SpSolver.m`.

The reference signal, the predicted signal and the model parameters c_k computed with `AutoReg` are shown in figure 14. Since the model computed with `AutoReg` has 1100 nonzero coefficients, the

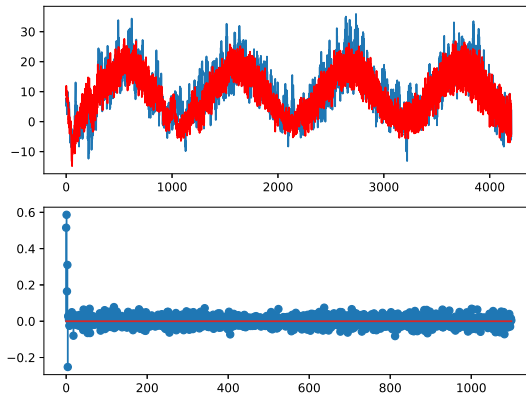


FIGURE 14. Reference signal (blue line) and model prediction (red line) (top). Model parameters computed using `AutoReg`. (bottom).

recurrence relation corresponding to the model computed with `AutoReg` will not be written explicitly.

The reference signal, the predicted signal and the model parameters c_k computed with algorithm 2 using `SINDy.m` are shown in figure 15.

The reference signal, the predicted signal and the model parameters c_k computed with algorithm 2 using `SpSolver.m` are shown in figure 16.

Although the models computed with `SpSolver.m` and `SINDy.m`, both have only 63 nonzero parameters c_k , we will not write the recurrence relations corresponding to these models explicitly either.

The root mean square error estimates for each model are documented in table 12, and the running times corresponding to the computation of the model parameters are documented in table 13.

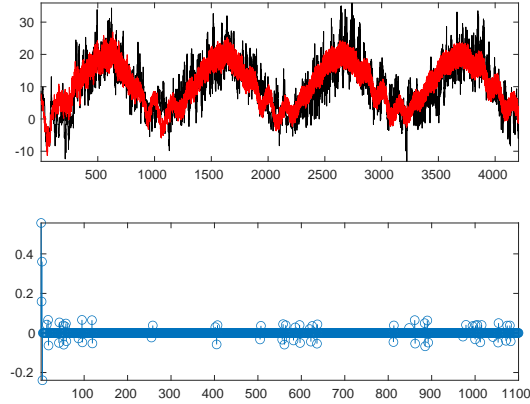


FIGURE 15. Reference signal (black line) and model prediction (red line) (top). Model parameters computed using `SINDy.m` (bottom).

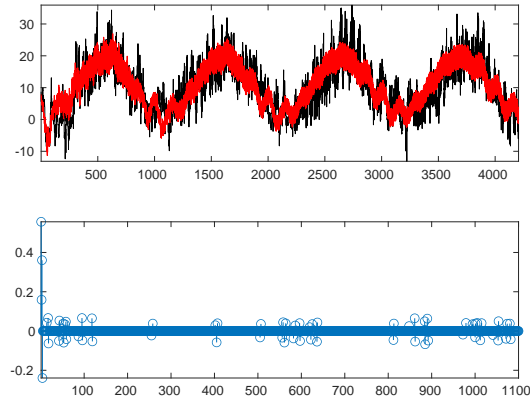


FIGURE 16. Reference signal (black line) and model prediction (red line) (top). Model parameters computed using `SpSolver.m` (bottom).

Method	RMSE
AutoReg	6.222
SINDy	5.8945
SDSI	5.8945

TABLE 12. Prediction error estimates corresponding to each method.

Method	Running Time (seconds)
AutoReg	1.0370969772338867
SINDy	0.896653
SDSI	0.562108

TABLE 13. Running times for the computation of the local linear model approximant.

The computational setting used for the experiments performed in this section is documented in the Matlab program `SpTSPredictor.m` and the Python program `TSPModel.py` in [31], these programs can be used to replicate these experiments.

6. CONCLUSION

The results in §3 and §4 in the form of algorithms like the ones described in §5.1, can be effectively used for the sparse identification of dynamical models that can be used to compute data-driven predictive numerical simulations.

One of the main advantages of the low-rank approximation approach presented in this document, concerns the parameter estimation for linear and nonlinear models where numerical or measurement noises could affect the estimates significantly, an example of this phenomenon is documented as part of the numerical experiment 5.2.1.

7. FUTURE DIRECTIONS

As a consequence of theorem 4.3, it is possible to approach system identification problems as approximate matrix completion problems via low-rank matrix approximation, the corresponding connections with local low-rank matrix approximation in the sense of [20] will be studied as part of the future directions of this research project.

As observed by Koch in [19], when applying sparse system identification techniques like the ones presented in this document, arriving at a high-quality model will be strongly related with the choice of functions in the method's library, which may require expert knowledge or tuning, and this consideration aligns perfectly with the philosophy behind the development of the system identification technology presented as part of the results reported in this article.

Computational implementations of the the sparse solvers and identification algorithms presented in this document to the computation of sparse signal models and signal compressions, using rectangular sparse submatrices of wavelet matrices, will also be the subject of future communications.

The connections of the results in §4 to the solution of problems related to controllability and realizability of finite-state systems in classical and quantum information and automata theory in the sense of [4, 2, 30, 5], will be further explored.

Further applications of sparse signal model identification schemes to industrial automation and building information modeling (BIM) technologies, will be further explored.

DATA AVAILABILITY

The programs and data that support the findings of this study are openly available in the SDSI repository, reference number [31].

CONFLICTS OF INTEREST

The author declares that he has no conflicts of interest.

ACKNOWLEDGMENT

The structure preserving matrix computations needed to implement the algorithms in §5.1, were performed with MATLAB R2021a (9.10.0.1602886) 64-bit (glnxa64), Python 3.8.5, Julia 1.6.0 and Netgen/NGSolve 6.2, with the support and computational resources of the Scientific Computing Innovation Center (**CICC-UNAH**) of the National Autonomous University of Honduras.

I am grateful with Terry Loring, Stan Steinberg, Concepción Ferrufino, Marc Rieffel and Moody Chu for interesting conversations, that have been very helpful for the preparation of this document.

REFERENCES

- [1] Rajendra Bhatia. *Matrix Analysis*, volume 169. Springer, 1997.
- [2] A. M. Bloch, R. W. Brockett, and C. Rangan. Finite controllability of infinite-dimensional quantum systems. *IEEE Transactions on Automatic Control*, 55(8):1797–1805, Aug 2010.
- [3] Christos Boutsidis and Malik Magdon-Ismail. A note on sparse least-squares regression. *Information Processing Letters*, 114(5):273–276, 2014.

- [4] R. Brockett and A. Willsky. Finite group homomorphic sequential system. *IEEE Transactions on Automatic Control*, 17(4):483–490, August 1972.
- [5] R. W. Brockett. Reduced complexity control systems. *IFAC Proceedings Volumes*, 41(2):1 – 6, 2008. 17th IFAC World Congress.
- [6] Steven L. Brunton, Joshua L. Proctor, and J. Nathan Kutz. Discovering governing equations from data by sparse identification of nonlinear dynamical systems. *Proceedings of the National Academy of Sciences*, 113(15):3932–3937, 2016.
- [7] Jie Chen, Haim Avron, and Vikas Sindhwani. Hierarchically compositional kernels for scalable nonparametric learning. *Journal of Machine Learning Research*, 18(66):1–42, 2017.
- [8] Francois Chollet. *Deep Learning with Python*. Manning Publications Co., USA, 1st edition, 2017.
- [9] J. J. Collins and I. N. Stewart. Coupled nonlinear oscillators and the symmetries of animal gaits. *Journal of Nonlinear Science*, 3(1), 1993.
- [10] J. J. Collins and I. N. Stewart. A group-theoretic approach to rings of coupled biological oscillators. *Biological Cybernetics*, 71(2), 1994.
- [11] M. Farhood and G. E. Dullerud. Lmi tools for eventually periodic systems. *Systems & Control Letters*, 47(5):417 – 432, 2002.
- [12] Marc Finzi, S. Stanton, Pavel Izmailov, and A. Wilson. Generalizing convolutional neural networks for equivariance to lie groups on arbitrary continuous data. In *ICML*, 2020.
- [13] John E. Franke and James F. Selgrade. Attractors for discrete periodic dynamical systems. *Journal of Mathematical Analysis and Applications*, 286(1):64–79, 2003.
- [14] Michael H. Freedman and William H. Press. Truncation of wavelet matrices: Edge effects and the reduction of topological control. *Linear Algebra and its Applications*, 234:1–19, 1996.
- [15] Gene H. Golub and Charles F. Van Loan. *Matrix Computations*. The Johns Hopkins University Press, Baltimore, 4th edition, 2013.
- [16] R. A. Horn. *Topics in Matrix Analysis*. Cambridge University Press, USA, 1986.
- [17] Kadierdan Kaheman, J. Nathan Kutz, and Steven L. Brunton. Sindy-pi: a robust algorithm for parallel implicit sparse identification of nonlinear dynamics. *Proceedings of the Royal Society A: Mathematical, Physical and Engineering Sciences*, 476(2242):20200279, 2020.
- [18] E. Kaiser, J. N. Kutz, and S. L. Brunton. Sparse identification of nonlinear dynamics for model predictive control in the low-data limit. *Proceedings of the Royal Society A: Mathematical, Physical and Engineering Sciences*, 474(2219):20180335, 2018.
- [19] J. Koch. Data-driven modeling of nonlinear traveling waves. *Chaos: An Interdisciplinary Journal of Nonlinear Science*, 31(4):043128, 2021.
- [20] Joonseok Lee, Seungyeon Kim, Guy Lebanon, Yoram Singer, and Samy Bengio. Llorma: Local low-rank matrix approximation. *J. Mach. Learn. Res.*, 17(1):442–465, January 2016.
- [21] Terry A. Loring and Fredy Vides. Computing floquet hamiltonians with symmetries. *Journal of Mathematical Physics*, 61(11):113501, 2020.
- [22] V. Moskvina and K. M. Schmidt. Approximate projectors in singular spectrum analysis. *SIAM Journal on Matrix Analysis and Applications*, 24(4):932–942, 2003.
- [23] J. L. Proctor, S. L. Brunton, and J. N. Kutz. Dynamic mode decomposition with control. *SIAM J Appl. Dyn. Syst.*, 15(1):142–161, 2016.
- [24] J.I. Ramos and F.R. Villatoro. The nonlinear schrödinger equation in the finite line. *Mathematical and Computer Modelling*, 20(3):31–59, 1994.
- [25] Fabio Della Rossa, Louis Pecora, Karen Blaha, Afroza Shirin, Isaac Klickstein, and Francesco Sorrentino. Symmetries and cluster synchronization in multilayer networks. *Nature Communications*, 11(1), 2020.
- [26] Anastasiya Salova, Jeffrey Emenheiser, Adam Rupe, James P. Crutchfield, and Raissa M. D’Souza. Koopman operator and its approximations for systems with symmetries. *Chaos: An Interdisciplinary Journal of Nonlinear Science*, 29(9):093128, 2019.
- [27] Hayden Schaeffer, Giang Tran, Rachel Ward, and Linan Zhang. Extracting structured dynamical systems using sparse optimization with very few samples. *Multiscale Modeling & Simulation*, 18(4):1435–1461, 2020.
- [28] P. J. Schmid. Dynamic mode decomposition of numerical and experimental data. *J. Fluid Mech.*, 656:5–28, 2010.
- [29] J. Schöberl. Netgen an advancing front 2d/3d-mesh generator based on abstract rules. *Computing and Visualization in Science*, 1:41–52, 1997.
- [30] D. C. Tarraf. An input-output construction of finite state ρ/μ approximations for control design. *IEEE Transactions on Automatic Control*, 59(12):3164–3177, Dec 2014.
- [31] F. Vides. SDSI: A toolset with matlab, python and julia programs for approximate sparse system identification, 2021. <https://github.com/FredyVides/SDSI>.
- [32] Rok Vrabič, John Ahmet Erkoyuncu, Peter Butala, and Rajkumar Roy. Digital twins: Understanding the added value of integrated models for through-life engineering services. *Procedia Manufacturing*, 16:139–146, 2018. Proceedings of the 7th International Conference on Through-life Engineering Services.

- [33] Louise Wright and Stuart Davidson. How to tell the difference between a model and a digital twin. *Advanced Modeling and Simulation in Engineering Sciences*, 7(1), 2020.

SCIENTIFIC COMPUTING INNOVATION CENTER, SCHOOL OF MATHEMATICS AND COMPUTER SCIENCE, UNIVERSIDAD NACIONAL AUTÓNOMA DE HONDURAS, TEGUCIGALPA, HONDURAS
Email address: `fredy.vides@unah.edu.hn`